Fujii T, Nagaya N, Iwase T, Murakami S, Miyahara Y, Nishigami K, Ishibashi-Ueda H, Shirai M, Itoh T, Ishino K, Sano S, Kangawa K, Mori H	Adrenomedullin enhances therapeutic potency of bone marrow transplantation for myocardial infarction in rats.	Am J Physiol Heart Circ Physiol	288	H1444-450	2004
Nagaya N, Kangawa K	Adrenomedullin in the treatment of pulmonary hypertension.	Peptides	25	2013-2018	2004
Takeno R, Okimura Y, Iguchi G, Kishimoto M, Kudo T, Takahashi K, Takahashi, Y, Kaji H, Ohno M, Ikuta H, Kuroda Y, Obara T, Hosoda H, Kangawa K, Chihara K	Intravenous administration of ghrelin stimulates growth hormone secretion in vagotomized patients as well as normal subjects.	Eur J Endocrinol	151	447-450	2004
Hanada R, Teranishi H, Pearson JT, Kurokawa M, Hosoda H, Fukushima N, Fukue Y, Serino R, Fujihara H, Ueta Y, Ikawa M, Okabe M, Murakami N, Shirai M, Yoshimatsu H, Kangawa K, Kojima M	Neuromedin U has a novel anorexigenic effect independent of the leptin signaling pathway.	Nat Med	10	1067-1073	2004
Itoh T, Nagaya N, Murakami S, Fujii T, Iwase T, Ishibashi-Ueda H, Yutani C, Yamagishi M, Kimura H, Kangawa K	C-Type natriuretic peptide ameliorates monocrotaline-induced pulmonary hypertension in rats.	Am J Respir Crit Care Med.	70	1204-11	2004
Takami Y, Horio T, Iwashima Y, Takiuchi S, Kamide K, Yoshihara F, Nakamura S, Nakahama H, Inenaga T, Kangawa K, Kawano Y	Diagnostic and prognostic value of plasma brain natriuretic peptide in non-dialysis-dependent CRF.	Am J Kidney Dis	44	420-428	2004
Murakami S, Nagaya N, Itoh T, Fujii T, Iwase T, Hamada K, Kimura H, Kangawa K	C-type natriuretic peptide attenuates bleomycin-induced pulmonary fibrosis in mice.	Am J Physiol Lung Cell Mol Physiol	287	L1172-1177	2004
Nagaya N, Fujii T, Iwase T, Ohgushi H, Itoh T, Uematsu M, Yamagishi M, Mori, Kangawa K, Kitamura S	Intravenous administration of mesenchymal stem cells improves cardiac function in rats with acute myocardial infarction through angiogenesis and myogenesis.	Am J Physiol Heart Circ Physiol	287	H2670-2676	2004
Nakamura R, Kato J, Kitamura K, Onitsuka H, Imamura T, Cao Y, Marutsuka K, Asada Y, Kangawa K, Eto T	Adrenomedullin administration immediately after myocardial infarction ameliorates progression of heart failure in rats.	Circulation	110	426-431	2004

Hino J, Kangawa K, Matsuo H, Nohno T, Nishimatsu S	Bone morphogenetic protein-3 family members and their biological functions.	Front Biosci	9	1520-1529	2004
Niu P, Shindo T, Iwata H, Iimuro S, Takeda N, Zhang Y, Ebihara A, Suematsu Y, Kangawa K, Hirata Y, Nagai R	Protective effects of endogenous adrenomedullin on cardiac hypertrophy, fibrosis, and renal damage.	Circulation	109	1789-1794	2004
Tokudome T, Horio T, Soeki T, Mori K, Kishimoto I, Suga S, Yoshihara F, Kawano Y, Kohno M, Kangawa K	Inhibitory effect of C-type natriuretic peptide (CNP) on cultured cardiac myocyte hypertrophy: interference between CNP and endothelin-1 signaling pathways.	Endocrinology	145	2131-2140	2004

雑誌　(小松弥郷)

発表者氏名	論文タイトル名	発表誌名	巻号	ページ	出版年
Ozasa A, Komatsu Y, Yasoda A, Miura M, Nakatsuru Y, Sakuma Y, Arai H, Itoh N, Nakao N	Complementary antagonistic actions between C-Type natriuretic peptide and MAPK pathway through FGFR-3 in ATDC5 cells.	Bone			in press
Majima T, Doi K, Komatsu Y, Itoh H, Fukao A, Shigemoto M, Takagi C, Corners J, Mizuta N, Kato R, Nakao K	Papillary thyroid carcinoma without metastases manifesting as an autonomously functioning thyroid nodule	Endocrin J			in press
Furuto-Kato S, Matsukura S, Ogata M, Azuma N, Manabe T, Shigeno C, Asato R, Tanaka K, Komatsu Y, Nakao K	Primary hyperparathyroidism presumably caused by chronic parathyroiditis manifesting from hypocalcemia to severe hypercalcemia.	Intern Med	44	60-64	2005
Majima T, Komatsu Y, Yamada T, Koike Y, Shigemoto M, Takagi C, Hatanaka I, Nakao K	Decreased bone mineral density at the distal radius, but not at the lumbar spine or the femoral neck, in Japanese type 2 diabetic patients.	Osteoporos Int			2004, Epub ahead of print.

Available online at www.sciencedirect.com
SCIENCE DIRECT
Journal of Molecular and Cellular Cardiology 38 (2005) 185–192
Journal of Molecular and Cellular Cardiology
www.elsevier.com/locate/yjmcc

Original Article

Hypertrophic responses to cardiotrophin-1 are not mediated by STAT3, but via a MEK5-ERK5 pathway in cultured cardiomyocytes

Nobuki Takahashi [a], Yoshihiko Saito [b,*], Koichiro Kuwahara [a], Masaki Harada [a], Keiji Tanimoto [a], Yasuaki Nakagawa [a], Rika Kawakami [a], Michio Nakanishi [a], Shinji Yasuno [a], Satoru Usami [a], Akihiko Yoshimura [c], Kazuwa Nakao [a]

[a] *Department of Medicine and Clinical Science, Kyoto University Graduate School of Medicine, Kyoto, Japan*
[b] *First Department of Internal Medicine, Nara Medical University, 840 Shijo-cho, Kashihara-city, Nara 634-8522, Japan*
[c] *Division of Molecular and Cellular Immunology, Medical Institute of Bioregulation, Kyushu University, Fukuoka, Japan*

Received 18 June 2004; received in revised form 3 October 2004; accepted 22 October 2004

Available online 10 December 2004

Abstract

gp130-dependent signaling is known to play a critical role in the onset of heart failure. In that regard, cardiotrophin-1 (CT-1) activates several signaling pathways via gp130, and induces hypertrophy in neonatal rat cardiomyocytes. Among the mediators activated by CT-1, STAT3 is thought to be important for induction of cell hypertrophy, though its precise function in the CT-1 signaling pathway is not fully understood. In the present study, therefore, to better understand the significance of STAT3 activity in CT-1 signaling, we infected cultured cardiomyocytes with adenoviral vectors harboring a dominant-negative STAT3 mutant or one of two endogenous negative regulators of cytokine signaling via the Janus kinase (JAK)-signal transducer and activator of transcription (STAT) pathways [suppressor of cytokine signaling (SOCS) 1 and 3] and then examined their effects on three indexes of CT-1-induced cell hypertrophy: protein synthesis, secretion of brain natriuretic peptide and changes in cell surface area. In control cells, CT-1-induced both STAT3 phosphorylation and cell hypertrophy. Overexpression of dominant-negative STAT3 mutant suppressed CT-1-induced STAT3 phosphorylation, but did not affect cell hypertrophy. On the other hand overexpression of SOCS1 or SOCS3 inhibited both CT-1-induced STAT3 phosphorylation and cell hypertrophy. CT-1 also induced phosphorylations of ERK1/2 and ERK5 in cardiomyocytes, and those, too, were suppressed by overexpression of SOCSs. CT-1-induced cell hypertrophy was suppressed by overexpression of a dominant-negative MEK5 mutant, and not by overexpression of a dominant-negative MEK1 mutant. These findings indicate that the major pathway responsible for the hypertrophic responses to CT-1 is not JAK-STAT3 pathway nor MEK1-ERK1/2 pathway, but MEK5-ERK5 pathway.

Keywords: Cardiotrophin-1; Cytokine; ERK1/2; ERK5; STAT3; Cell signaling; Hypertrophy; Cardiomyocyte

1. Introduction

Cardiotrophin-1 (CT-1) is an interleukin-6 (IL-6)-related cytokine that exerts various hypertrophic and antiapoptotic effects via the gp130-leukemia inhibitory factor (LIF) receptor complex by activating several intracellular signaling in cardiomyocytes, including the Janus kinase (JAK)-signal transducer and activator of transcription (STAT) and mitogen-activated protein kinase (MAPK) pathways [1]. The receptors for IL-6-related cytokines share gp130 as a signal-transducing receptor component [1]. Its continuous activation in heart due, for example, to overexpression of IL-6 and its receptor is known to cause myocardial hypertrophy [2]. Conversely, ventricular restricted gp130-deficient mice display massive apoptosis of cardiomyocytes and are unable to achieve compensatory hypertrophy during aortic pressure overload [3]. So it is very important to elucidate the physi-

Abbreviations: BNP, brain natriuretic peptide; CT-1, cardiotrophin-1; ERK, extracellular signal-regulated kinase; ET-1, endothelin-1; GPCR, G-protein-coupled receptor; IL-6, interleukin-6; JAK, Janus kinase; LIF, leukemia inhibitory factor; MAPK, mitogen-activated protein kinase; MEK, MAPK/ERK kinase; PI3K, phosphatidylinositol 3-OH kinase; SOCS, suppressor of cytokine signaling; STAT, signal transducer and activator of transcription.

* Corresponding author. Tel.: +81-744-29-8850; fax: +81-744-22-9726.
E-mail address: yssaito@nmu-gw.naramed-u.ac.jp (Y. Saito).

0022-2828/$ - see front matter © 2004 Elsevier Ltd. All rights reserved.
doi:10.1016/j.yjmcc.2004.10.016

ological or pathophysiological role of IL-6-related cytokines in the heart.

On the other hand, little is known about the significance of the signaling pathways downstream of gp130 that mediates the phenotypic, namely hypertrophic and antiapoptotic effects of IL-6-related cytokines such as CT-1. We previously showed that CT-1 induces its antiapoptotic effects via the phosphatidylinositol 3-OH kinase (PI3K)-Akt pathway [4]. In addition, others have shown that LIF, which shares a receptor with CT-1, induces hypertrophy in cardiomyocytes via STAT3 [5], and that cardiac-specific overexpression of STAT3 leads to myocardial hypertrophy [6]. In those cases, however, the contribution made by STAT3 did not appear especially pronounced, making it unclear whether STAT3 mediated transduction in the principal pathway leading to hypertrophy. In that regard, we have shown that CT-1-induced STAT3 activation leads to upregulation of two endogenous negative regulators of cytokine signaling via JAK-STAT pathways [suppressor of cytokine signaling (SOCS) 1 and 3, also referred to as JAK-binding protein (JAB) and cytokine-inducible SH2 protein (CIS) 3/STAT-induced STAT inhibitor (SSI) 1and 3] [7–9] in the heart [10].

Finally, Kodama et al. [11] have shown that the MAPK/extracellular signal-regulated kinase (ERK) kinase (MEK)1/2-ERK1/2 pathway is critically involved in LIF-induced cardiomyocyte hypertrophy. Moreover, Nicol et al. [12] recently reported that in cardiomyocytes LIF activates ERK5, a novel member of the MAPK family, and that a dominant-negative form of MEK5, the MAPK kinase directly responsible for activation of ERK5, inhibits LIF-induced elongation of cardiomyocytes.

With those as background, we hypothesized that the major molecule responsible for the hypertrophic responses to IL-6-related cytokines may not be STAT3, but ERK1/2 or ERK5. So in this study, we examined the effects of overexpressing SOCSs, dominant-negative mutant of STAT3, MEK1 or MEK5 on CT-1-induced cardiomyocyte hypertrophy with the aim of better understanding the significance of the STAT3 and MEK-ERK pathways in CT-1-induced cardiac hypertrophy.

2. Materials and methods

2.1. Materials

Recombinant rat CT-1 was prepared using a GST-fusion system (Pharmacia Biotechnology, Inc.) according to the manufacturer's instructions. Human endothelin-1 (ET-1) was purchased from Peptide Institute. Anti-STAT3, anti-phospho-STAT3 (Tyr705), anti-p44/42 MAPK (ERK1/2), anti-phospho-ERK1/2 (Thr202/Tyr204) and anti-phospho-ERK5 (Thr218/Tyr220) antibodies were from Cell Signaling Technology. Anti-ERK5/BMK1 antibody was from Upstate Biotechnology. Anti-SOCS3/CIS3 antibody was from Immuno-Biological Laboratories. PD98059 was from Calbiochem.

2.2. Recombinant adenoviruses

Adenoviral vectors harboring the genes for LacZ (Ad-LacZ), myc-tagged SOCS1 (AdSOCS1), myc-tagged SOCS3 (AdSOCS3), an HA-tagged dominant-negative STAT3 mutant (AdSTAT3F) in which phosphorylation-site Tyr705 was substituted with Phe [13], and Cre recombinase (AdCre) were gifts from Dr. Yasushi Hanakawa, Ehime University School of Medicine, Ehime, Japan [14]; an adenoviral vector containing the gene for a dominant-negative MEK5 mutant (AdMEK5KM) in which ATP-binding Lys106 was substituted with Met [15] was a gift from Dr. Eric N. Olson, University of Texas, Dallas, USA [12]; and an adenoviral vector harboring the gene for a dominant-negative MEK1 mutant (AdMEK1DN) in which Asp208 in the kinase subdomain VII was substituted with an Ala [16] was a gift from Dr. Seinosuke Kawashima, Kobe University, Kobe, Japan. Because of the toxic effect of SOCS1 on 293 cells used for recombinant virus production, a Cre-LoxP conditional expression system was employed to generate AdSOCS1 using the protocol described by Kanegae et al. [17]. For that reason, only AdSOCS1 was co-infected with AdCre. All adenoviral vectors harbor the cytomegalovirus enhancer and the chicken β-actin promoter.

2.3. Cardiomyocyte culture and adenovirus infection

Ventricular myocytes were prepared from 1-day-old Wistar rats using a Percoll gradient as previously described [18]. The investigation conforms to the Guiding Principles in the Care and Use of Animals (American Physiological Society). After collecting the myocytes from the gradient, they were preplated on noncoated dishes for 1 h, after which the unattached cells were collected; this cell population consisted of >97% myocytes as assessed by immunofluorescence with anti-rat sarcomeric actin antibody (DAKO Japan Co., Ltd.). The myocytes were then plated on gelatin-coated dishes in serum-containing medium for 24 h. The medium was then replaced with serum-free medium, and the cells were infected for 24 h with one of the recombinant adenoviruses at a multiplicity of infection (MOI) of 10 viral particles per cell. Under these conditions, >99% of the myocytes were infected (assessed by X-gal staining or immunocytochemistry with anti-tag antibodies). Thereafter, the cells were treated with 10^{-9} mol/l CT-1 or 10^{-8} mol/l ET-1 for the indicated times. In some cases, the MEK inhibitor PD98059 was applied for 30 min prior to addition of CT-1 or ET-1.

2.4. Western blot analysis

After incubating the cells with CT-1 or ET-1 for the indicated times, they were washed with ice-cold phosphate-buffered saline (PBS) and lyzed with lysis buffer (Cell Signaling Technology). The resultant whole-cell protein extracts were subjected to 10% SDS-PAGE, and the resolved proteins were electrophoretically transferred onto polyvinylidene dif-

luoride membranes (Bio-Rad Laboratories). The membranes were then blocked with 5% skim milk (Difco Laboratories) and probed with the indicated antibodies.

2.5. Analysis of protein synthesis in cultured cells

Protein synthesis in cultured cardiomyocytes was evaluated using [^{3}H]-leucine incorporation as an index. Following incubation with CT-1 or ET-1, the cells were cultured for 24 h, after which 3 μCi of [^{3}H]-leucine (Amersham Life Science) was added for an additional 24 h. After washing twice with ice-cold PBS, the cells were incubated in 10% trichloroacetic acid for 30 min at 4 °C. The resultant precipitate was solubilized in 0.2 N NaOH for >4 h, and the radioactivity was measured in a liquid scintillation counter.

2.6. Radioimmunoassay for brain natriuretic peptide

Levels of brain natriuretic peptide (BNP) in medium conditioned for 48 h by cardiomyocytes after stimulation with CT-1 or ET-1 was measured using a specific radioimmunoassay as previously described [19].

2.7. Statistical analysis

Data are presented as mean ± standard deviations (S.D.) of results of four independent experiments. Unpaired Student's *t*-tests were used to determine significant differences between two groups, and ANOVA with post hoc Fisher's tests was used to determine significant differences among three or four groups. Values of $P < 0.05$ were considered significant.

3. Results

3.1. Effects of SOCSs and STAT3F on CT-1-induced STAT3 phosphorylation

First, to determine whether SOCSs are the true endogenous negative regulators of CT-1 signaling in our cultured cardiomyocytes, Western blot analysis was carried out using samples from CT-1-treated cardiomyocytes probed with anti-SOCS3 antibody. As shown in Fig. 1A, upregulation of SOCS3 protein was confirmed in CT-1-treated cardiomyocytes. We previously showed that CT-1 induced tyrosine phosphorylation of STAT3 in cardiomyocytes, and that the response peaked within 5–15 min of CT-1 application [20]. Next, therefore, we examined the effects of overexpressing SOCS1, SOCS3 and STAT3F on levels of STAT3 tyrosine phosphorylation after 10 min of CT-1 stimulation. AdSOCS1, AdSOCS3 and AdSTAT3F did not have an influence on the basal phosphorylation of STAT3 (Fig. 1B). As shown in Figs. 1B, and 1C, CT-1 induced substantial phosphorylation of STAT3 in cardiomyocytes infected with AdLacZ. This effect was completely blocked in cardiomyocytes infected with AdSOCS1 or AdSOCS3, and significantly inhibited in

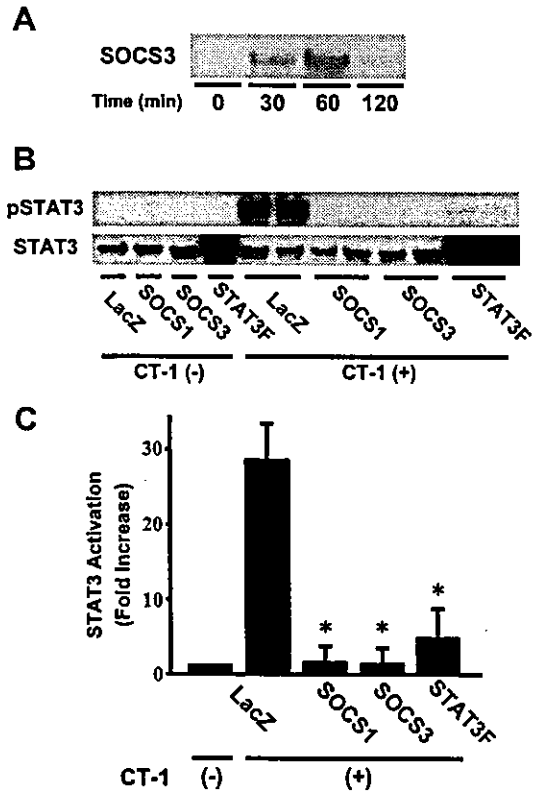

Fig. 1. SOCS3 expression induced by CT-1 and effects of SOCS1, SOCS3 and STAT3F on CT-1-induced phosphorylation of STAT3. (A) Representative Western blots showing the time course SOCS3 protein expression in CT-1-treated cardiomyocytes without adenovirus infection. (B) Representative Western blots showing the effects of SOCS1, SOCS3 and STAT3F on CT-1-induced phosphorylation of STAT3. Cardiomyocytes infected with AdLacZ, AdSOCS1, AdSOCS3 or AdSTAT3F were treated with 10^{-9} mol/L CT-1 for 10 minutes, after which cell lysates were harvested. (C) Phospho-STAT3 (pSTAT3) and STAT3 were measured densitometrically from immunoblots like those in panel B. The ratio of pSTAT3 to STAT3 was normalized to that in AdLacZ-infected cardiomyocytes without CT-1 treatment, which was assigned a value of 1. Only in regard to AdSTAT3F-infected group, the ratio to the average STAT3 of the other adenovirus-infected groups was used. Values are means ± S.D. (n = 8) of four independent experiments, each experiment performed with two distinct samples; $^*P < 0.01$ vs. LacZ with CT-1.

cardiomyocytes infected with AdSTAT3F. The apparently augmented expression of STAT3 in cardiomyocytes infected with AdSTAT3F reflects the cross-reaction of anti-STAT3 antibody with overexpressed STAT3F, and is indicative of the efficiency of the protein expression in cardiomyocytes transfected using these recombinant adenoviral vectors.

3.2. Effects of SOCSs and STAT3F on CT-1-induced cardiomyocyte hypertrophy

We next examined the effects of overexpressing SOCS1, SOCS3 or STAT3F on CT-1-induced hypertrophy of cardiomyocytes. For comparison, ET-1, a G-protein-coupled receptor (GPCR) agonist, was also used to induce a distinct form of cardiomyocyte hypertrophy [21]. We first evaluated CT-1- and ET-1-induced [^{3}H]-leucine incorporation as an index of protein synthesis. As shown in Fig. 2A, CT-1 significantly increased [^{3}H]-leucine incorporation in cardiomyocytes

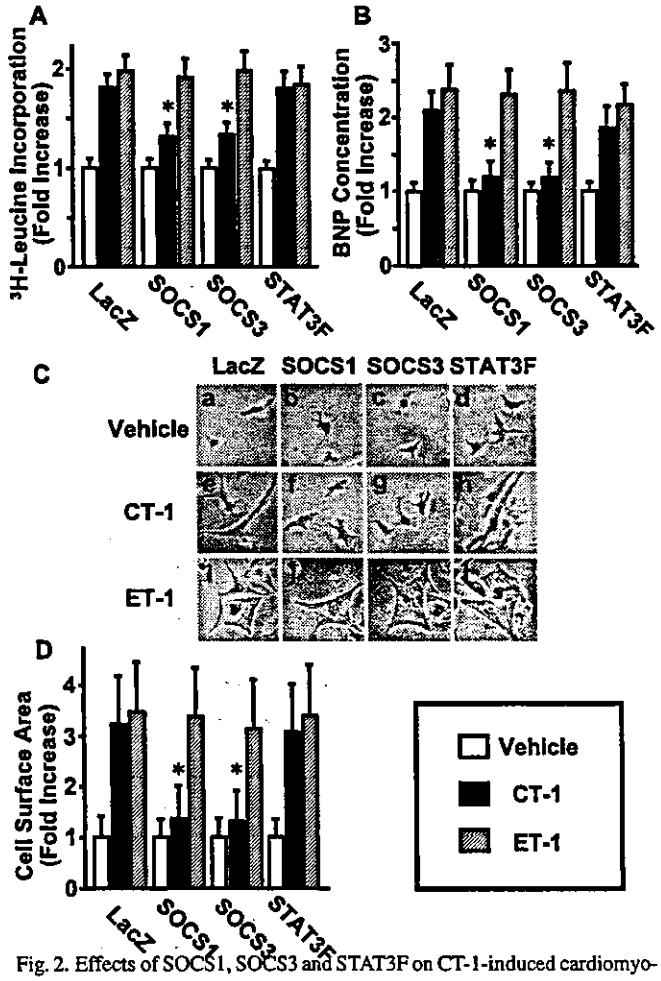

Fig. 2. Effects of SOCS1, SOCS3 and STAT3F on CT-1-induced cardiomyocyte hypertrophy. Cardiomyocytes infected with AdLacZ, AdSOCS1, AdSOCS3 or AdSTAT3F were treated with vehicle (open bars), 10^{-9} mol/L CT-1 (solid bars) or 10^{-8} mol/L ET-1 (hatched bars). The fold increase is relative to vehicle-treated cells of each adenovirus-infected group. (A) ^{3}H-leucine incorporation by cardiomyocytes during the period from 24 to 48 hours after treatment. (B) BNP concentration in the cultured media 48 hours after treatment. (C) Phase-contrast photographs of cultured cardiomyocytes taken 48 hours after treatment with vehicle *(a-d)*, CT-1 *(e-h)* or ET-1 *(i-l)*. (D) Cell surface areas were analyzed using NIH Image software. A total of 100 cells were examined for each group. The experiments were repeated four times independently, and each was performed with six distinct samples (A, B). Values are means ± S.D. (n = 24 in A and B, n = 100 in D); $^*P < 0.05$ vs. LacZ with CT-1.

infected with AdLacZ. This effect was significantly inhibited by infection with AdSOCS1 or AdSOCS3 but, somewhat surprisingly, not by infection with AdSTAT3F. Infection with AdSOCS1, AdSOCS3 or AdSTAT3F had no effect on ET-1-induced [^{3}H]-leucine incorporation.

The effects of AdSOCS1, AdSOCS3 and AdSTAT3F on BNP secretion from cardiomyocytes paralleled their effects on [^{3}H]-leucine incorporation (Fig. 2B)—i.e. infection with AdSOCS1 or AdSOCS3 significantly inhibited CT-1-induced BNP secretion, whereas infection with AdSTAT3F did not. ET-1-induced BNP secretion was unaffected by AdSOCS1, AdSOCS3 or AdSTAT3F.

CT-1- and ET-1-induced cardiomyocyte hypertrophy was also examined by evaluating their effect on cell shape and surface area. Consistent with an earlier report [21], CT-1 induced a characteristic hypertrophy in cardiomyocytes infected with AdLacZ (Fig. 2Ce)—i.e. it elicited pronounced increases in cell length, but did not significantly affect the width. ET-1, by contrast, elicited increases in both cell length and width (Fig. 2Ci). Infection with AdSOCS1 or AdSOCS3 (Fig. 2Cf, g and 2D), but not AdSTAT3F (Fig. 2Ch and 2D), inhibited CT-1-induced changes in cell shape and size. ET-1-induced changes in cell shape and size were unaffected by AdSOCS1, AdSOCS3 or AdSTAT3F (Fig. 2Cj-l and 2D).

3.3. Effects of SOCSs and STAT3F on CT-1-induced ERK phosphorylation

Collectively, the results presented so far indicate that inhibition of STAT3 alone does not inhibit CT-1-induced cardiomyocyte hypertrophy. Only when SOCSs are used to inhibit other signaling pathways is the hypertrophy inhibited. In that regard, CT-1 is known to also induce activation of ERK1/2 in cardiomyocytes [1], while LIF, another IL-6-related cytokine, has been reported to induce activation of ERK5 in cardiomyocytes [12]. With that in mind, we examined the effects of overexpressing SOCS1, SOCS3 or STAT3F on CT-1-induced activation (phosphorylation) of ERK1/2 and ERK5. AdSOCS1, AdSOCS3 and AdSTAT3F did not affect the basal phosphorylation of ERK1/2 nor ERK5 (Fig. 3D). We found that CT-1-induced phosphorylation of both ERK1/2 and ERK5 that peaked within ~10 min (Fig. 3A–C), and these effects were significantly inhibited by infection with AdSOCS1 or AdSOCS3, but not AdSTAT3F (Fig. 3D–F). Thus, the effects of overexpressing SOCS1, SOCS3 or STAT3F on CT-1-induced ERK activation differed from the effects on STAT3 activation, but paralleled the effects on cardiomyocyte hypertrophy.

3.4. Effects of PD98059 on CT-1-induced ERK phosphorylation and on CT-1-induced cardiomyocyte hypertrophy

The MEK1 inhibitor PD98059 [22] was recently shown to also inhibit MEK5, the specific upstream activator of ERK5, though at a somewhat higher concentration [23]. Likewise, we found that PD98059 concentration-dependently inhibited CT-1-induced phosphorylation of both ERK1/2 and ERK5, but that it was a more potent inhibitor of the former (Fig. 4A–C). PD98059 also inhibited both CT-1- and ET-1-induced [^{3}H]-leucine incorporation and BNP secretion (Fig. 4D, E). It is noteworthy that the potency of the inhibitory effect of PD98059 on the activities of CT-1 and ET-1 paralleled the potency of its effect on the phosphorylation of ERK5 and ERK1/2, respectively.

3.5. Effects of dominant-negative MEK1 and MEK5 mutants on CT-1-induced cardiomyocyte hypertrophy

The results obtained with PD98059 were confirmed when we examined the effects of overexpressing dominant-negative

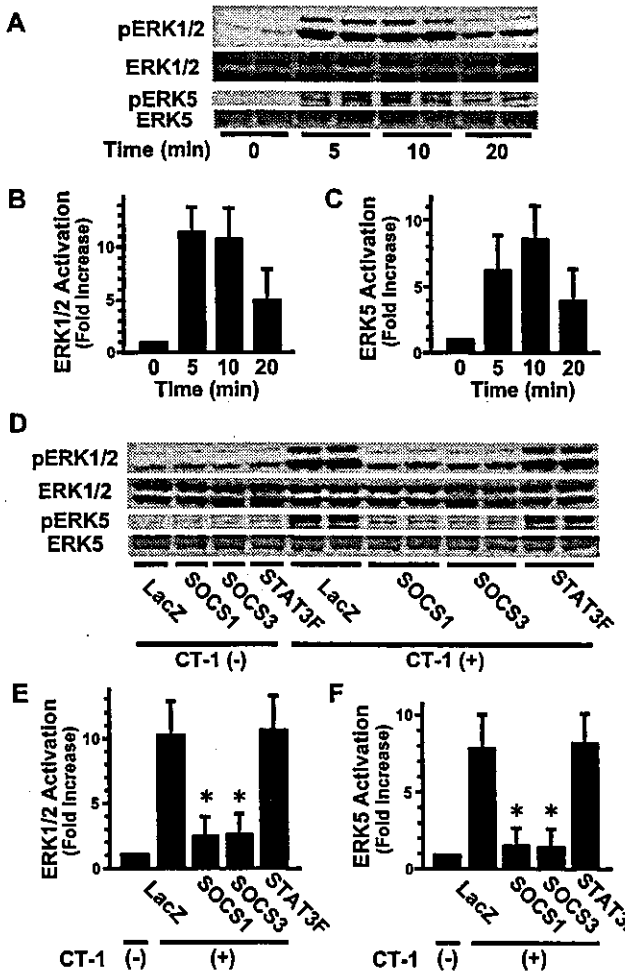

Fig. 3. Time course of CT-1-induced phosphorylation of ERK1/2 and ERK5, and effects of SOCS1, SOCS3 and STAT3F on CT-1-induced phosphorylation of ERK1/2 and ERK5. (A) Representative Western blots showing the time course of CT-1-induced phosphorylation of ERK1/2 and ERK5. Cardiomyocytes infected with AdLacZ were stimulated with 10^{-9} mol/L CT-1 for the indicated times, after which cell lysates were harvested. (B) Phospho-ERK1/2 (pERK1/2) and ERK1/2 were measured densitometrically from immunoblots like those in panel A. The ratio of pERK1/2 to ERK1/2 was normalized to that in cardiomyocytes without CT-1 treatment, which was assigned a value of 1. (C) Phospho-ERK5 (pERK5) and ERK5 were analyzed as panel B. (D) Representative Western blots showing the effects of SOCS1, SOCS3 and STAT3F on CT-1-induced phosphorylation of ERK1/2 and ERK5. Cardiomyocytes infected with AdLacZ, AdSOCS1, AdSOCS3 or AdSTAT3F were treated with 10^{-9} mol/L CT-1 for 10 min, after which the cell lysates were harvested. (E) Phospho-ERK1/2 (pERK1/2) and ERK1/2 were measured densitometrically from immunoblots like those in panel D. The ratio of pERK1/2 to ERK1/2 was normalized to that in AdLacZ-infected cardiomyocytes without CT-1 treatment, which as assigned a value of 1. (F) Phospho-ERK5 (pERK5) and ERK5 were analyzed in the same way as panel E. Values are means ± S.D. (n = 8) of four independent experiments, each experiment performed with two distinct samples; *$P < 0.05$ vs. LacZ with CT-1.

MEK1 or MEK5 mutants on CT-1-induced phosphorylation of ERKs and cardiomyocyte hypertrophy. As shown in Fig. 5, infection with AdMEK1DN inhibited both the basal phosphorylation of ERK1/2 and CT-1-induced phosphorylation of ERK1/2, but did not have an influence on the phosphorylation of ERK5. On the other hand, infection with AdMEK5KM inhibited both the basal phosphorylation of

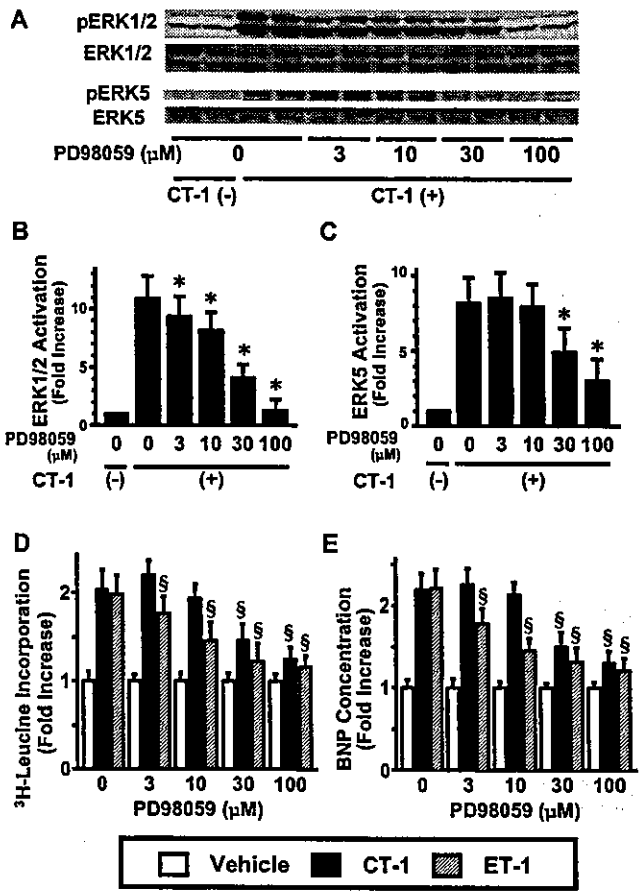

Fig. 4. Effects of PD98059 on CT-1-induced phosphorylation of ERK1/2 and ERK5 and CT-1- and ET-1-induced cardiomyocyte hypertrophy. Cardiomyocytes cultured with the indicated concentration of PD98059 were treated with vehicle (open bars), 10^{-9} mol/L CT-1 (solid bars) or 10^{-8} mol/L ET-1 (hatched bars). (A) Representative Western blots of phospho-ERK1/2 (pERK1/2) and phospho-ERK5 (pERK5) in lysates harvested after 10 minutes of CT-1 treatment. (B) pERK1/2 and ERK1/2 were measured densitometrically from immunoblots like those in panel A. The ratio of pERK1/2 to ERK1/2 was normalized to that in cardiomyocytes without CT-1 treatment, which as assigned a value of 1. (C) pERK5 and ERK5 were analyzed in the same way as panel B. (D) ^{3}H-leucine incorporation by cardiomyocytes during the period from 24 to 48 hours after treatment. (E) BNP concentration in the cultured media 48 hours after treatment. Fold increase is relative to vehicle-treated cells in each concentration group. The experiments were repeated four times independently, and each was performed with two distinct samples (A-C) or with sis distinct samples (D, E). Values are means ± S.D. (n = 8 in A to C, n = 24 in D and E); *$P < 0.05$ vs. PD98059 (-) with CT-1, §$P < 0.05$ vs. LacZ with CT-1 or ET-1, correspondently.

ERK5 and CT-1-induced phosphorylation of ERK5, but did not have an influence on the phosphorylation of ERK1/2. And as shown in Fig. 6, infection with AdMEK5KM but not AdMEK1DN significantly inhibited CT-1-induced increases in [^{3}H]-leucine incorporation, BNP secretion and cell surface area. Conversely, infection with AdMEK1DN but not AdMEK5KM inhibited the ET-1-induced effects.

4. Discussion

The aim of the present study was to assess the significance of the STAT3 and MEK-ERK pathways in CT-1-induced

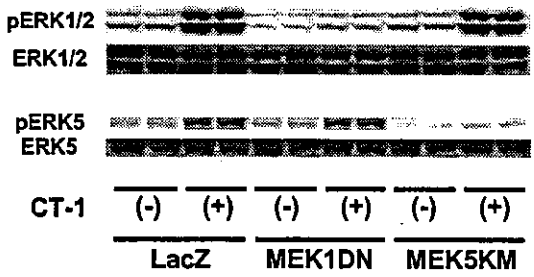

Fig. 5. Effects of dominant-negative MEK1 (MEK1DN) and MEK5 (MEK5KM) mutants on CT-1-induced phosphorylation of ERK1/2 and ERK5. Representative Western blots of phospho-ERK1/2 (pERK1/2) and phospho-ERK5 (pERK5) in lysates harvested after 10 minutes of CT-1 treatment.

hypertrophy of cultured neonatal rat ventricular myocytes. Among several pathways activated by IL-6-related cytokines in cardiomyocytes, the STAT3 pathway is reportedly important for mediating cardiomyocyte hypertrophy [5,6,24]. In our study, however, a dominant-negative STAT3 mutant did not inhibit CT-1-induced cardiomyocyte hypertrophy, although it suppressed activation (phosphorylation) of STAT3. We can not explain strictly the discrepancy of our results from previous study [5], but we think that it may be attributable to the difference of culture conditions, for example the degree of fibroblasts contamination. We have confirmed the existence of STAT3 in cardiac fibroblasts and its phosphorylation induced by CT-1 (data not shown). With the results in our study, the major pathway leading from CT-1 binding to the gp130 complex to cardiomyocyte hypertrophy is not via STAT3. On the other hand, two recently identified [7–9] endogenous negative regulators of cytokine signaling via JAK-STAT pathways, SOCS1 and SOCS3, significantly inhibited both STAT3 phosphorylation and the hypertrophic effects of CT-1, which is consistent with an earlier report [14]. In addition, SOCS1/3 and dominant-negative STAT3 mutant had the same influence on the hypertrophic effects of LIF, another member of IL-6-related cytokines (data not shown), indicating that these differential effects of SOCSs vs. dominant-negative STAT3 are not CT-1 specific, but shared with other members of IL-6-related cytokines. The key question then was what gp130-dependent signaling pathway do SOCSs suppress to inhibit CT-1-induced hypertrophy?

Among the possibilities are the STAT1 pathway [25], the PI3K-Akt pathway [26] and the MEK1/2-ERK1/2 pathway [11,16], all of which appear to be involved in LIF-induced cardiomyocyte hypertrophy. The first two are easily ruled out. We found that dominant-negative STAT3 inhibited CT-1-induced phosphorylation of not only STAT3 but also STAT1 (data not shown), most likely because STAT3 and STAT1 share docking sites for JAK1/2 [1]. Therefore, if CT-1 acted via STAT1, we would expect its effects to have been inhibited by the dominant-negative STAT3 mutant. As for the PI3K-Akt pathway, we previously showed that this pathway is largely responsible for CT-1's antiapoptotic effects rather than cell hypertrophy [4].

This leaves the MEK-ERK pathways. PD98059 is known as a specific inhibitor of MEK1 [22], but some reports suggest that it also inhibits MEK5 at a somewhat higher concentration [23,27]. Consistent with those results, we found that at concentrations <30 μM PD98059 selectively inhibits evoked ERK1/2 phosphorylation and ET-1-induced cardiomyocyte hypertrophy. At concentrations ≥30 μM, however, PD98059 also inhibits ERK5 phosphorylation and CT-1-induced cardiomyocyte hypertrophy. On the other hand, it is also known that PD98059 loses specificity at the higher concentrations. So we added the examinations with dominant-negative MEK1 or MEK5 mutant to confirm our hypothesis acquired from the examinations with PD98059. Dominant-negative MEK1 mutant partially inhibited ET-1-induced hypertrophy, but had not effect on CT-1-induced hypertro-

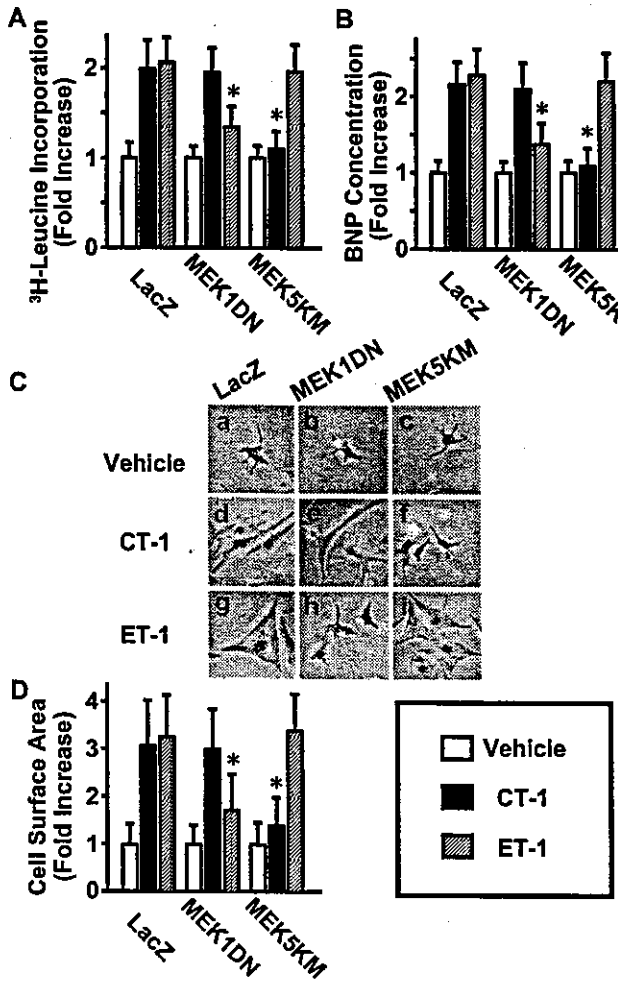

Fig. 6. Effects of dominant-negative MEK1 (MEK1DN) and MEK5 (MEK5KM) mutants on CT-1-induced cardiomyocyte hypertrophy. Cardiomyocytes infected with AdLacZ, AdMEK1DN or AdMEK5KM were treated with vehicle (open bars), 10^{-9} mol/L CT-1 (solid bars) or 10^{-8} mol/L ET-1 (hatched bars). The fold increase is relative to vehicle-treated cells in each adenovirus-infected group. **(A)** ^{3}H-leucine incorporation by cardiomyocytes during the period from 24 to 48 hours after treatment. **(B)** BNP concentration in the cultured media 48 hours after treatment. **(C)** Phase-contrast photographs of cultured cardiomyocytes obtained 48 hours after treatment with vehicle *(a-c)*, CT-1 *(d-f)* or ET-1 *(g-i)*. **(D)** Cell surface areas were analyzed using NIH Image software. A total of 100 cells were examined for each group. The experiments were repeated four times independently, and each was performed with six distinct samples (**A, B**). Values are means ± S.D. (n = 24 in A and B, n = 100 in D); $^*P < 0.05$ vs. LacZ with CT-1.

phy, whereas dominant-negative MEK5 mutant almost completely inhibited CT-1-induced hypertrophy, but had no effect on ET-1-induced hypertrophy. We therefore conclude that CT-1-induced cardiomyocyte hypertrophy is mediated mainly via a MEK5-ERK5 pathway, while ET-1-induced hypertrophy is at least partially via a MEK1/2-ERK1/2 pathway. The fact that SOCSs inhibited CT-1-induced phosphorylation of ERK5 indicates they suppress hypertrophic responses to CT-1 through inhibition of a MEK5-ERK5 pathway. These conclusions are further supported by the findings that gp130-deficient [28] and ERK5-deficient mice [29] show similar embryonic cardiovascular defects, suggesting ERK5 is an important mediator situated downstream of gp130 during cardiovascular development.

CT-1-induced cardiomyocyte hypertrophy is distinct from that induced by GPCR agonists including ET-1 and angiotensin II [21]. Pathophysiological significance of GPCR agonists in the heart is undoubted because of the clinical usefulness of angiotensin-converting-enzyme (ACE) inhibitors [30–33]. On the other hand, there is little clinical evidence concerning IL-6-related cytokines including CT-1. With regard to mouse models, however, IL-6-related cytokines are known to induce concentric hypertrophy via gp130 in in vivo heart [2]. Although here we have shown the significance of the MEK5-ERK5 pathway in cardiomyocyte hypertrophy induced by CT-1, a member of IL-6-related cytokines, activated MEK5 has been shown to induce eccentric, not concentric, hypertrophy in in vivo heart [12]. That is to say, activation of only a MEK5-ERK5 pathway can not account for the cardiac phenotype induced by IL-6-related cytokines. Several signaling pathways including JAK-STATs, MEK-ERKs and PI3K-Akt pathways probably cooperate and express the cardiac phenotype induced by IL-6-related cytokines. So it is necessary to investigate more detailed role of not only a MEK5-ERK5 pathway, but also the other signaling pathways downstream of gp130 in the cardiomyocyte or in the heart stimulated with IL-6-related cytokines. Furthermore, it is expected to elucidate the clinical significance of IL-6-related cytokines in the heart.

Finally, our finding that the MEK5-ERK5 pathway plays a critical role in CT-1-induced cardiomyocyte hypertrophy raises the question, what is the role of STAT3 in cardiomyocytes? Kunisada et al. [6] reported that STAT3 transduces a protective signal against doxorubicin-induced cardiomyopathy, but we detected no related phenotypes in cardiomyocytes overexpressing a dominant-negative STAT3 mutant. It may be that the key role played by STAT3 in cardiomyocytes involves the induction of SOCSs [10] and subsequent inhibition of the MEK5-ERK5 pathway.

Acknowledgments

This work was supported in part by research grants from the Japanese Ministry of Education, Culture, Sports, Science and Technology, the Japanese Ministry of Health, Labor and Welfare, and the Research for the Future Program of the Japan Society for the Promotion of Science (JSPS-RFTF96I00204 and 98L00801), and by grants from the Japanese Cardiovascular Research Foundation, Uehara Memorial Foundation and the Smoking Research Foundation. We thank Dr. E. Olson, Dr. S. Kawashima and Dr. Y. Hanakawa for providing adenovirus vectors and thanks to K. Okamura for her excellent secretarial work.

References

[1] Wollert KC, Chien KR. Cardiotrophin-1 and the role of gp130-dependent signaling pathways in cardiac growth and development. J Mol Med 1997;75:492–501.

[2] Hirota H, Yoshida K, Kishimoto T, Taga T. Continuous activation of gp130, a signal-transducing receptor component for interleukin 6-related cytokines, causes myocardial hypertrophy in mice. Proc Natl Acad Sci USA 1995;92:4862–8.

[3] Hirota H, Chen J, Betz UA, Rajewsky K, Gu Y, Ross Jr. J, et al. Loss of a gp130 cardiac muscle cell survival pathway is a critical event in the onset of heart failure during biomechanical stress. Cell 1999;97:189–98.

[4] Kuwahara K, Saito Y, Kishimoto I, Miyamoto Y, Harada M, Ogawa E, et al. Cardiotrophin-1 phosphorylates akt and BAD, and prolongs cell survival via a PI3K-dependent pathway in cardiac myocytes. J Mol Cell Cardiol 2000;32:1385–94.

[5] Kunisada K, Tone E, Fujio Y, Matsui H, Yamauchi-Takihara K, Kishimoto T. Activation of gp130 transduces hypertrophic signals via STAT3 in cardiac myocytes. Circulation 1998;98:346–52.

[6] Kunisada K, Negoro S, Tone E, Funamoto M, Osugi T, Yamada S, et al. Signal transducer and activator of transcription 3 in the heart transduces not only a hypertrophic signal but a protective signal against doxorubicin-induced cardiomyopathy. Proc Natl Acad Sci USA 2000;97:315–9.

[7] Starr R, Willson TA, Viney EM, Murray LJ, Rayner JR, Jenkins BJ, et al. A family of cytokine-inducible inhibitors of signalling. Nature 1997;387:917–21.

[8] Endo TA, Masuhara M, Yokouchi M, Suzuki R, Sakamoto H, Mitsui K, et al. A new protein containing a SH2 domain that inhibits JAK kinases. Nature 1997;387:921–4.

[9] Naka T, Narazaki M, Hirata M, Matsumoto T, Minamoto S, Aono A, et al. Structure and function of a new STAT-induced STAT inhibitor. Nature 1997;387:924–9.

[10] Hamanaka I, Saito Y, Yasukawa H, Kishimoto I, Kuwahara K, Miyamoto Y, et al. Induction of JAB/SOCS-1/SSI-1 and CIS3/SOCS-3/SSI-3 is involved in gp130 resistance in cardiovascular system in rat treated with cardiotrophin-1 in vivo. Circ Res 2001;88:727–32.

[11] Kodama H, Fukuda K, Pan J, Sano M, Takahashi T, Kato T, et al. Significance of ERK cascade compared with JAK/STAT and PI3-K pathway in gp130-mediated cardiac hypertrophy. Am J Physiol Heart Circ Physiol 2000;279:H1635–H1644.

[12] Nicol RL, Frey N, Pearson G, Cobb M, Richardson J, Olson EN. Activated MEK5 induces serial assembly of sarcomeres and eccentric cardiac hypertrophy. EMBO J 2001;20:2757–67.

[13] Minami M, Inoue M, Wei S, Takeda K, Matsumoto M, Kishimoto T, et al. STAT3 activation is a critical step in gp130-mediated terminal differentiation and growth arrest of a myeloid cell line. Proc Natl Acad Sci USA 1996;93:3963–6.

[14] Yasukawa H, Hoshijima M, Gu Y, Nakamura T, Pradervand S, Hanada T, et al. Suppressor of cytokine signaling-3 is a biomechanical stress-inducible gene that suppresses gp130-mediated cardiac myocyte hypertrophy and survival pathways. J Clin Invest 2001;108:1459–67.

[15] English JM, Pearson G, Hockenberry T, Shivakumar L, White MA, Cobb MH. Contribution of the ERK5/MEK5 pathway to Ras/Raf signaling and growth control. J Biol Chem 1999;274:31588–92.

[16] Ueyama T, Kawashima S, Sakoda T, Rikitake Y, Ishida T, Kawai M, et al. Requirement of activation of the extracellular signal-regulated kinase cascade in myocardial cell hypertrophy. J Mol Cell Cardiol 2000;32:947–60.

[17] Kanegae Y, Lee G, Sato Y, Tanaka M, Nakai M, Sakaki T, et al. Efficient gene activation in mammalian cells by using recombinant adenovirus expressing site-specific Cre recombinase. Nucleic Acids Res 1995;23:3816–21.

[18] Harada M, Itoh H, Nakagawa O, Ogawa Y, Miyamoto Y, Kuwahara K, et al. Significance of ventricular myocytes and nonmyocytes interaction during cardiocyte hypertrophy: evidence for endothelin-1 as a paracrine hypertrophic factor from cardiac nonmyocytes. Circulation 1997;96:3737–44.

[19] Nakao K, Ogawa Y, Suga S, Imura H. Molecular biology and biochemistry of the natriuretic peptide system. I: natriuretic peptides. J Hypertens 1992;10:907–9012.

[20] Kuwahara K, Saito Y, Harada M, Ishikawa M, Ogawa E, Miyamoto Y, et al. Involvement of cardiotrophin-1 in cardiac myocyte–nonmyocyte interactions during hypertrophy of rat cardiac myocytes in vitro. Circulation 1999;100:1116–24.

[21] Wollert KC, Taga T, Saito M, Narazaki M, Kishimoto T, Glembotski CC, et al. Cardiotrophin-1 activates a distinct form of cardiac muscle cell hypertrophy. Assembly of sarcomeric units in series VIA gp130/leukemia inhibitory factor receptor-dependent pathways. J Biol Chem 1996;271:9535–45.

[22] Alessi DR, Cuenda A, Cohen P, Dudley DT, Saltiel AR. PD 098059 is a specific inhibitor of the activation of mitogen-activated protein kinase kinase in vitro and in vivo. J Biol Chem 1995;270:27489–94.

[23] Kamakura S, Moriguchi T, Nishida E. Activation of the protein kinase ERK5/BMK1 by receptor tyrosine kinases. Identification and characterization of a signaling pathway to the nucleus. J Biol Chem 1999; 274:26563–71.

[24] Railson JE, Liao Z, Brar BK, Buddle JC, Pennica D, Stephanou A, et al. Cardiotrophin-1 and urocortin cause protection by the same pathway and hypertrophy via distinct pathways in cardiac myocytes. Cytokine 2002;17:243–53.

[25] Kodama H, Fukuda K, Pan J, Makino S, Baba A, Hori S, et al. Leukemia inhibitory factor, a potent cardiac hypertrophic cytokine, activates the JAK/STAT pathway in rat cardiomyocytes. Circ Res 1997;81:656–63.

[26] Oh H, Fujio Y, Kunisada K, Hirota H, Matsui H, Kishimoto T, et al. Activation of phosphatidylinositol 3-kinase through glycoprotein 130 induces protein kinase B and p70 S6 kinase phosphorylation in cardiac myocytes. J Biol Chem 1998;273:9703–10.

[27] Mody N, Leitch J, Armstrong C, Dixon J, Cohen P. Effects of MAP kinase cascade inhibitors on the MKK5/ERK5 pathway. FEBS Lett 2001;502:21–4.

[28] Yoshida K, Taga T, Saito M, Suematsu S, Kumanogoh A, Tanaka T, et al. Targeted disruption of gp130, a common signal transducer for the interleukin 6 family of cytokines, leads to myocardial and hematological disorders. Proc Natl Acad Sci USA 1996;93:407–11.

[29] Regan CP, Li W, Boucher DM, Spatz S, Su MS, Kuida K. Erk5 null mice display multiple extraembryonic vascular and embryonic cardiovascular defects. Proc Natl Acad Sci USA 2002;99:9248–53.

[30] The CONSENSUS Trial Study Group. Effects of enalapril on mortality in severe congestive heart failure. Results of the Cooperative North Scandinavian Enalapril Survival Study (CONSENSUS). N Engl J Med 1987;316:1429–35.

[31] The SOLVD Investigators. Effect of enalapril on survival in patients with reduced left ventricular ejection fractions and congestive heart failure. N Engl J Med 1991;325:293–302.

[32] Swedberg K, Held P, Kjekshus J, Rasmussen K, Ryden L, Wedel H. Effects of the early administration of enalapril on mortality in patients with acute myocardial infarction. Results of the Cooperative New Scandinavian Enalapril Survival Study II (CONSENSUS II). N Engl J Med 1992;327:678–84.

[33] The SOLVD Investigators. Effect of enalapril on mortality and the development of heart failure in asymptomatic patients with reduced left ventricular ejection fractions. N Engl J Med 1992;327:685–91.

0013-7227/05/$15.00/0
Printed in U.S.A.

Endocrinology 146(1):355–364

doi: 10.1210/en.2004-0629

Transgenic Mice Overexpressing Des-Acyl Ghrelin Show Small Phenotype

Hiroyuki Ariyasu, Kazuhiko Takaya, Hiroshi Iwakura, Hiroshi Hosoda, Takashi Akamizu, Yuji Arai, Kenji Kangawa, and Kazuwa Nakao

Department of Medicine and Clinical Science (H.A., K.N.), Kyoto University Graduate School of Medicine, and Translational Research Center (K.T., H.I., H.H., T.A., K.K.), Kyoto University Hospital, Kyoto 606-8507; and Departments of Bioscience (Y.A.) and Biochemistry (K.K.), National Cardiovascular Center Research Institute, Osaka 565-8565, Japan

Ghrelin, a 28-amino acid acylated peptide, displays strong GH-releasing activity in concert with GHRH. The fatty acid modification of ghrelin is essential for the actions, and des-acyl ghrelin, which lacks the modification, has been assumed to be devoid of biological effects. Some recent reports, however, indicate that des-acyl ghrelin has effects on cell proliferation and survival. In the present study, we generated two lines of transgenic mice bearing the preproghrelin gene under the control of chicken β-actin promoter. Transgenic mice overexpressed des-acyl ghrelin in a wide variety of tissues, and plasma des-acyl ghrelin levels reached 10- and 44-fold of those in control mice. They exhibited lower body weights and shorter nose-to-anus lengths, compared with control mice. The serum GH levels tended to be lower, and the serum IGF-I levels were significantly lower in both male and female transgenic mice than control mice. The responses of GH to administered GHRH were normal, whereas those to administered ghrelin were reduced, especially in female transgenic mice, compared with control mice. These data suggest that overexpressed des-acyl ghrelin may modulate the GH-IGF-I axis and result in small phenotype in transgenic mice. (*Endocrinology* 146: 355–364, 2005)

GHRELIN, AN ACYLATED peptide of 28 amino acids, was identified as an endogenous ligand for the GH secretagogue (GHS) receptor (GHS-R) (1). The major site of production of ghrelin is the stomach and it is also expressed in the hypothalamus (2–5). Plasma ghrelin levels are regulated by acute feeding states. They rise by fasting and are rapidly suppressed by feeding (3, 6–8). Secretion of ghrelin is also regulated by chronic feeding states. Plasma ghrelin levels are elevated in patients with anorexia nervosa and food-restricted animals and are reduced in obese subjects (3, 6–10). These data suggest the possible involvement of ghrelin in energy homeostasis. In fact, ghrelin stimulates food intake in animals and humans and exhibits anticachectic effect in cancer-bearing mice (8, 11–13).

Exogenously administered ghrelin strongly stimulates GH release in a clear dose-dependent manner *in vivo* (1, 2, 14–16). The site of ghrelin action on GH release is not well known to date. The GHS-R is reported to be expressed in the pituitary as well as hypothalamus (17–19). Previous studies indicate that ghrelin binds to membranes from the pituitary and stimulates GH release from cultured pituitary cells (1, 20), suggesting that the pituitary is one of the sites of ghrelin actions. The stimulatory effect of GHSs and ghrelin on GH secretion, however, is more prominent *in vivo* than *in vitro*, and intact GHRH signaling is essential for the effect (1, 21). Hexarelin, one of the potent GHSs, cannot efficiently stimulate GH release in patients with GHRH receptor deficiency (22). Moreover, as we demonstrated, ghrelin has a synergistic action with GHRH. Even a low dose of ghrelin can highly augment GH release by GHRH (23). These data indicate a critical role of the hypothalamus in the stimulatory effect of ghrelin on GH secretion. The strong potency of ghrelin suggests its role as a physiological regulator of GH secretion (1, 2, 14–16). The issue, however, is currently controversial. One recent study (24), using a GHS antagonist, revealed that circulating ghrelin in peripheral blood may not play a role in generating pulsatile GH secretion. Moreover, deletion of ghrelin impairs neither growth nor appetite, indicating that ghrelin is not critically required for GH secretion (25). Another study (26), however, demonstrated that the attenuation of the GHS-R expression *in vivo* results in reduction in food intake and growth, suggesting a physiological role of the ghrelin-GHS-R system in the secretory regulation of GH.

The acylation of ghrelin is assumed to be essential for its actions (1). Des-acyl ghrelin, which lacks the fatty acid modification and circulates at 10-fold higher concentration than acylated ghrelin (1, 3, 27), is devoid of any endocrine activities including GH release, based on previous studies (1, 28). Recent studies (29, 30), however, indicated that des-acyl ghrelin may share with acylated ghrelin the modulation of neoplastic cell proliferation and cardiovascular cell survival *in vitro*. Moreover, one study shows that des-acyl ghrelin may offset the inhibitory effect of acylated ghrelin on insulin secretion (28). Although previous studies indicated that several tissues and cell lines produce des-acyl and/or acylated ghrelin (3, 27, 31, 32), the mechanism by which ghrelin is acylated is also unknown to date.

In the present study, we generated transgenic mice bearing the preproghrelin gene under the control of a cytomegalovirus immediate early enhancer and a modified chicken β-

First Published Online October 7, 2004

Abbreviations: BMI, Body mass index; GHS, GH secretagogue; GHS-R, GHS receptor.

Endocrinology is published monthly by The Endocrine Society (http://www.endo-society.org), the foremost professional society serving the endocrine community.

actin promoter, designated CAG promoter (33, 34). This promoter sequence has been demonstrated to have high activity in cultured cells and transgenic mice (33, 34). Transgenic mice in the present study overexpressed des-acyl ghrelin in plasma and a wide variety of tissues and showed small phenotype. Here we show that des-acyl ghrelin may modulate endogenous ghrelin action and alter the GH-IGF-I axis in transgenic mice.

Materials and Methods

All procedures in animal experiments were approved by the Kyoto University Graduate School of Medicine Committee on Animal Research. The procedures were performed in accordance with the principle and guidelines established by the committee.

Plasmid construction and generation of transgenic mice

The full-length mouse preproghrelin cDNA (1) and the pCAGGS expression vector including the CAG promoter (34) were kindly donated by Professor Masayasu Kojima (Division of Molecular Genetics, Institute of Life Science, Kurume University, Kurume, Japan) and Professor Junichi Miyazaki (Department of Nutrition and Physiological Chemistry, Osaka University School of Medicine, Osaka, Japan), respectively. Plasmid pCAGGS-ghrelin was constructed by inserting the mouse preproghrelin cDNA into the unique *Eco*RI site between the CAG promoter and 3′-flanking sequence of the rabbit β-globin gene of the pCAGGS expression vector. The DNA fragment was excised from its plasmid by digestion with *Sal*I and *Hind*III and then purified and microinjected into the pronuclei of fertilized eggs obtained from BDF1 female mice (Charles River Japan, Yokohama, Japan) as reported previously (35). Founder transgenic mice were identified by PCR analysis and bred with C57BL/6 mice (Japan CLEA, Osaka, Japan). Mice were housed in air-conditioned animal quarters, with the lights on between 0800 and 2000 h and were given standard rat chow (CE-2, 352 kcal per 100 g, Japan CLEA) and water *ad libitum*.

Measurement of total and acylated ghrelin levels in tissue samples

Tissues such as the stomach, cerebrum, heart, and kidney were removed from 8-wk-old mice under anesthesia with diethyl ether. Each sample was diced and boiled for 7 min in a 5-fold volume of water. The solution was adjusted to 1.0 M acetic acid and 20 mM hydrogen chloride after boiling, and the tissue was homogenized. The supernatant was obtained after centrifugation at 10,000 rpm for 30 min. Tissue ghrelin levels were measured using two kinds of RIAs, C-RIA for the carboxyl terminal and N-RIA for the amino terminal of ghrelin as reported previously (9, 27). C-RIA and N-RIA recognize total (acylated plus des-acyl ghrelin) and acylated ghrelin, respectively (9, 27).

Measurement of plasma total and acylated ghrelin levels

Blood samples were collected from the inferior vena cava of mice under anesthesia with diethyl ether. The samples were immediately transferred to chilled polypropylene tubes containing Na_2EDTA (1 mg/ml) and aprotinin (Ohkura Pharmaceutical, Inc., Kyoto, Japan; 1000 kallikrein inactivator U/ml) and centrifuged at 4 C. For N-RIA, hydrogen chloride was added to the samples at final concentration of 0.1 N immediately after the separation of plasma. Plasma ghrelin was measured as reported previously (1, 3, 27). Briefly, the samples were subjected to a Sep-Pak C18 cartridge and C-RIA and N-RIA were carried out.

Measurement of body weights and lengths, organ weights, and daily food intake

Body weights of control and transgenic mice were measured weekly, beginning at 3 wk of age. Body lengths of 8- and 52-wk-old mice were measured by manual immobilization and extension of mice to the nose-to-anus lengths, always by the same individual. Body mass indexes (BMIs = weight/(nose-to-anus lengths)^2) were calculated in 8- and 52-wk-old control and transgenic mice (36, 37). Organs such as the pituitary, stomach, cerebrum, heart, liver, kidney, spleen, pancreas, and epididymal fat were removed from 8-wk-old mice under anesthesia with diethyl ether and weighed. Daily food intake was monitored for 3 wk, beginning at 5 wk of age.

Measurement of blood glucose, serum total protein, total cholesterol, and hormones

To examine the nutritional conditions, blood glucose and serum total protein and total cholesterol levels were measured. Eight-week-old control and transgenic mice were used. Four hundred microliters of blood samples were collected from the tail vein of mice for blood glucose levels at 1000 h after 12 h fasting. Then the mice were anesthetized with diethyl ether, and 400 μl of blood samples were collected from the inferior vena cava for serum total protein, total cholesterol, and hormone levels. Blood glucose, serum total protein, and total cholesterol levels were measured by the glucose oxidase method with a reflectance glucometer (One Touch II; Lifescan, Milpitas, CA), BCA protein assay reagent kit (Pierce, Rockford, IL), and Amplex red cholesterol assay kit (Molecular Probes, Eugene, OR), respectively. Serum GH and IGF-I levels were measured with EIA kits (SPI-BIO, Bonde, France, and Diagnostic Systems Laboratories Inc., Webster, TX, respectively). Serum insulin and plasma ACTH levels were measured with EIA kits (Morinaga, Tokyo, Japan) and ACTH-RIA kit (Nichols Institute Diagnostics, San Juan Capistrano, CA), respectively. Serum TSH, LH, and FSH levels were measured with EIA kits (Amersham Biosciences, Buckinghamshire, UK).

Effects of GHRH and ghrelin on serum GH levels

Human GHRH and rat ghrelin were purchased from Sumitomo Pharmaceuticals Co., Ltd. (Osaka, Japan) and Peptide Institute, Inc. (Osaka, Japan), respectively. Male and female 8-wk-old control and Tg 10–1 mice were used under no anesthesia. Control and transgenic mice were housed in the same cage and tested on the same day. Forty mice were divided into five groups for blood sampling. Eight mice in the same group were used for each blood sampling. Control and transgenic mice were iv injected with human GHRH (60 μg/kg) or rat ghrelin (40 μg/kg). Four hundred microliters of blood samples were collected from the inferior vena cava of mice 0, 10, 20, 30, and 60 min after the injection. Serum GH levels were measured with an EIA kit (SPI-BIO).

Real-time PCR analysis of preproghrelin, GH, GHRH, somatostatin, and GHS-R mRNAs

Total RNAs from tissues, such as the stomach, small intestine, cerebrum, hypothalamus, pituitary, liver, kidney, lung, heart, and skeletal muscle, were extracted using the acid guanidinium thiocyanate-phenol-chloroform method (38). First-strand cDNA was synthesized from 1 μg of total RNA using Superscript II RT (Life Technologies, Inc., St. Louis, MO) with random hexamers according to the manufacturer's instructions. Taqman-PCR was performed with the ABI Prism 7700 sequence detection system (Applied Biosystems, Foster City, CA) using VIC-labeled fluorogenic probes specific for preproghrelin, GH, GHRH, somatostatin, or GHS-R transcript, or the internal standard glyceraldehyde-3-phosphate dehydrogenase. Oligo primers and probes (Table 1) were chosen using the Primer Express software (Applied Biosystems). The PCR was performed using Taqman Universal PCR Mastermix (Applied Biosystems) to which primers and probes were added (final concentrations 400 and 200 nM, respectively). All samples were run in triplicate in 96-well plates in the ABI Prism 7700 sequence detector according to the manufacturer's standard protocol. For the primer sets, serial dilutions were conducted with different cDNA preparations to confirm the kinetics of the PCR. There was no significant difference in glyceraldehyde-3-phosphate dehydrogenase mRNA levels among experimental groups.

Effects of continuous infusion of des-acyl ghrelin on the GH-IGF-I axis and body weights

Rat des-acyl ghrelin was purchased from Peptide Institute, Inc. Des-acyl ghrelin was dissolved in saline at a concentration of 700 μg/ml and stored in osmotic minipumps (DURECT Corp., Cupertino, CA). The

TABLE 1. Primer and probe sequences for real-time PCR analysis for preproghrelin, GH, GHRH, somatostatin, and GHS-R mRNAs

	Primer and probe sequences
Preproghrelin	
Forward	5′-GCATGCTCTGGATGGACATG-3′
Reverse	5′-TGGTGGCTTCTTGGATTCCT-3′
Probe	5′-AGCCCAGAGCACCAGAAAGCCCA-3′
GH	
Forward	5′-AAGAGTTCGAGCGTGCCTACA-3′
Reverse	5′-GAAGCAATTCCATGTCGGTTC-3′
Probe	5′-CCATTCAGAATGCCCAGGCTGCTTTC-3′
GHRH	
Forward	5′-AGGATGCAGCGACACGTAGA-3′
Reverse	5′-TCTCCCCTTGCTTGTTCATGA-3′
Probe	5′-CCACCAACTACAGGAAACTCCTGAGCCA-3′
Somatostatin	
Forward	5′-AGCTGAGCAGGACGAGATGAG-3′
Reverse	5′-ACAGGATGTGAATGTCTTCCAGAA-3′
Probe	5′-CGAACCCAGCAATGGCACCCC-3′
GHS-R	
Forward	5′-CACCAACCTCTACCTATCCAGCAT-3′
Reverse	5′-CTGACAAACTGGAAGAGTTTGCA-3′
Probe	5′-TAAGATCTGCTCATCTTAATGTGCATG-3′

minipumps were implanted into the peritoneum. Des-acyl ghrelin or saline was infused continuously through the minipumps into 4-wk-old C57/BL6 mice (Japan CLEA) for 10 d. The minipumps were continuously delivering saline or 250 μg/kg·d of des-acyl ghrelin for 10 d at a speed of 0.22 μl/h. Body weights were measured daily for 10 d. Four hundred microliters of blood samples for the measurement of serum GH and IGF-1 levels were collected from the inferior vena cava of mice under anesthesia with diethyl ether 10 d after the implantation.

Hematoxylin eosin and immunohistochemical staining for total ghrelin, acylated ghrelin, and GH of the pituitary

The pituitaries were removed from male 8-wk-old mice under anesthesia with diethyl ether and fixed with 4% paraformaldehyde and 0.2% picric acid and embedded in paraffin. The tissues were cut in 3-μm-thick slices. Samples were subjected to immunohistochemical staining for total and acylated ghrelin as well as hematoxylin eosin staining. After pretreatment with 0.3% hydrogen peroxide and incubation with normal goat serum, all slices were incubated overnight at 4 C with ghrelin(13–28) antiserum recognizing total (des-acyl plus acylated) ghrelin (final dilution, 1:5000), antighrelin(1–11) antiserum specifically recognizing acylated ghrelin (final dilution, 1:5000), or anti-GH antiserum (Biogenesis, Poole, UK) (final dilution, 1:200). All of the sections were stained by the avidin-biotin complex method and counterstained with hematoxylin as reported previously (39).

Statistical analysis

Results are expressed as the mean ± SEM. ANOVA followed by the *t* test was used to assess differences between control and transgenic mice. $P < 0.05$ was considered to be statistically significant.

Results

Generation of transgenic mice and preproghrelin mRNA levels

Two lines of transgenic mice with six (Tg 10–1) and 12 (Tg 9–2) copy numbers were identified by PCR and Southern blot analysis. Preproghrelin mRNAs were detected only in the stomach, small intestine, lung, pituitary, and hypothalamus of control mice, and the amounts were 100, 4, 2.1, 1.5, and 0.5 in arbitrary units (AU), respectively (Fig. 1). On the other hand, they were detected in all tissues examined in Tg 9–2 and Tg 10–1 mice, and the amounts in the stomach of Tg 9–2 and Tg 10–1 mice reached 1100 and 5200 AU, respectively (Fig. 1). Preproghrelin mRNA levels in other tissues of Tg 9–2 and Tg 10–1 mice also exceeded those of control mice.

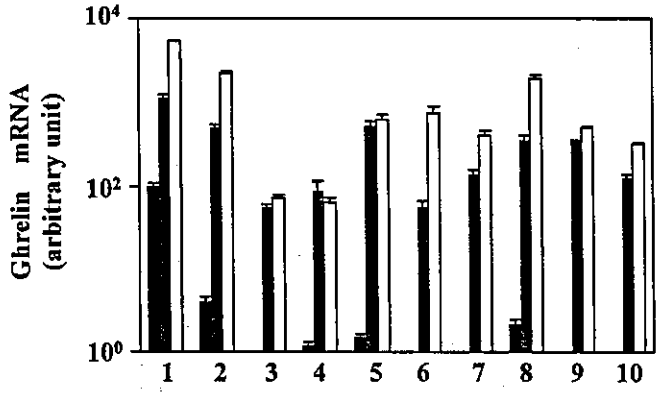

FIG. 1. Preproghrelin mRNA levels in the tissues of control (*closed bars*), Tg 9–2 (*shaded bars*), and Tg 10–1 (*open bars*) mice quantified by real-time PCR analysis. Lanes 1, stomach; 2, small intestine; 3, cerebrum; 4, hypothalamus; 5, pituitary; 6, liver; 7, kidney; 8, lung; 9, heart; and 10, skeletal muscle.

Total and acylated ghrelin levels in tissues and plasma

Eight-week-old control, Tg 9–2, and Tg 10–1 mice were used (Table 2). Although high total ghrelin levels were detected in the stomach, only very low levels were detected in other tissues of control mice. Tg 9–2 and Tg 10–1 mice showed significantly higher total ghrelin levels in the stomach than control mice ($P < 0.01$ for each). Tg 9–2 and Tg 10–1 mice also showed total ghrelin levels in all of the other tissues significantly higher than control mice. High levels of acylated ghrelin were also detected in the stomach of control, Tg 9–2, and Tg 10–1 mice. There was, however, no significant difference between control and Tg 9–2 mice and between control and Tg 10–1 mice. Only very low acylated ghrelin levels if any were detected in other tissues of control, Tg 9–2, and Tg 10–1 mice. Plasma total ghrelin levels in control, Tg 9–2, and Tg 10–1 mice were 1104.5 ± 94.4, 11230.6 ± 1147.1, and 48565.5 ± 9291.5 fmol/ml, respectively. Those in Tg 9–2 and Tg 10–1 mice were significantly higher than those in control mice ($P < 0.01$ for each). Plasma acylated ghrelin levels in control, Tg 9–2, and Tg 10–1 mice were 83.7 ± 11.9, 79.7 ± 10.1, and 86.3 ± 21.1 fmol/ml, respectively. The differences between control and Tg 9–2 mice and control and Tg 10–1 mice were not significant.

Body weights and lengths, relative organ weights, and BMIs

Body weights of control, Tg 9–2, and Tg 10–1 mice are shown in Table 3 and Fig. 2A. Male Tg 9–2 and Tg 10–1 mice were significantly lighter in the body weight than control mice ($P < 0.05$ and $P < 0.01$, respectively). Female Tg 10–1 mice were also significantly lighter than control mice ($P < 0.01$). The difference between female control and Tg 9–2 mice was not significant. Fifteen-week-old male and female Tg 10–1 and male Tg 9–2 mice were still significantly lighter than control mice ($P < 0.05$, $P < 0.01$, and $P < 0.01$, respectively). Body lengths (nose-to-anus lengths) of control and

TABLE 2. Total and acylated ghrelin levels in plasma and tissues of 8-wk-old control and transgenic mice (n = 8/group)

	Control	Tg 9-2	Tg 10-1
Total ghrelin			
Plasma (fmol/ml)	1104.5 ± 94.4	11230.6 ± 1147.1[a]	48565.5 ± 9291.5[a]
Tissues (fmol/mg)			
Stomach	2191.9 ± 340.9	2860.8 ± 587.3[a]	5430.6 ± 626.1[a]
Cerebrum	0.8 ± 0.2	34.3 ± 4.2[a]	110.9 ± 41.0[a]
Heart	1.4 ± 0.2	27.6 ± 5.6[a]	30.2 ± 9.3[a]
Kidney	1.9 ± 0.1	43.5 ± 5.9[a]	68.3 ± 10.5[a]
Acylated ghrelin			
Plasma (fmol/ml)	83.7 ± 11.9	79.7 ± 10.6	86.3 ± 21.1
Tissues (fmol/mg)			
Stomach	413.0 ± 46.7	341.2 ± 66.8	325.0 ± 49.5
Cerebrum	0.05>	0.05>	0.05>
Heart	0.1 ± 0.0	0.05>	0.05>
Kidney	0.1 ± 0.0	0.1 ± 0.1	0.1 ± 0.0

Values are given as the mean ± SEM.
[a] $P < 0.01$ *vs.* control mice.

transgenic mice are shown in Table 3. Eight-week-old male Tg 9–2 and Tg 10–1 mice were significantly shorter in the body length than control mice ($P < 0.05$ and $P < 0.01$, respectively). Female Tg 10–1 mice were significantly shorter than control mice ($P < 0.01$). The difference between female control and Tg 9–2 mice was not significant. BMIs were calculated from the body weights and lengths. No significant difference was noted between control and Tg 9–2 mice and control and Tg 10–1 mice (Table 3). Fifty-two-week-old male Tg 9–2 and Tg10–1 mice were still significantly lighter and shorter, compared with control mice (Table 3), and no significant difference was noted in BMIs between control and transgenic mice. Relative organ weights of 8-wk-old male control and Tg 10–1 mice were calculated from the organ and body weights. No significant difference was noted between control and Tg 10–1 mice (Fig. 2B). No significant difference was noted in the pituitary size between control and Tg 10–1 mice (0.058 ± 0.002 and 0.055 ± 0.003 mg/body weight (grams), respectively).

TABLE 3. Body weights, lengths, and BMIs of 8-wk-old and 52-wk-old control and transgenic mice (n = 8/group)

		Control	Tg 9-2	Tg 10-1
Male				
8-wk-old	Body weight (g)	23.2 ± 0.5	21.0 ± 0.7[a]	16.6 ± 0.6[b]
	Nose-to-anus length (cm)	9.2 ± 0.3	8.6 ± 0.1[a]	7.7 ± 0.3[b]
	BMI (g/cm^2)	27.1 ± 1.2	28.1 ± 3.1[c]	27.3 ± 1.9[c]
52-wk-old	Body weight (g)	34.7 ± 0.8	31.2 ± 0.6[a]	28.4 ± 0.1[b]
	Nose-to-anus length (cm)	10.1 ± 0.1	9.5 ± 0.3[a]	9.1 ± 0.1[b]
	BMI (g/cm^2)	34.4 ± 0.8	34.7 ± 0.6[c]	34.5 ± 0.8[c]
Female				
8-wk-old	Body weight (g)	16.6 ± 1.2	18.7 ± 0.7[c]	10.7 ± 1.1[b]
	Nose-to-anus length (cm)	8.1 ± 0.6	8.5 ± 0.2[c]	6.4 ± 0.2[b]
	BMI (g/cm^2)	25.8 ± 1.8	26.2 ± 1.2[c]	26.5 ± 1.5[c]
52-wk-old	Body weight (g)	25.3 ± 1.3	24.8 ± 0.8[c]	19.6 ± 0.7[b]
	Nose-to-anus length (cm)	9.0 ± 0.4	8.9 ± 0.3[c]	7.9 ± 0.2[b]
	BMI (g/cm^2)	30.9 ± 1.0	31.2 ± 0.7[c]	31.3 ± 1.1[c]

Values are given as the mean ± SEM.
[a] $P < 0.05$ *vs.* control mice.
[b] $P < 0.01$ *vs.* control mice.
[c] Not significant.

Immunohistochemical staining for total and acylated ghrelin of the pituitary

Immunohistochemical staining for total and acylated ghrelin is shown in Fig. 3, A–D. None of total ghrelin-positive cells were observed in the pituitary of control mice (Fig. 3A). On the other hand, many total ghrelin-immunoreactive pituitary cells were observed in Tg 10–1 mice (Fig. 3B). Approximately 30% of the anterior pituitary cells in all sections examined were total ghrelin immunoreactive. None of acylated ghrelin-positive cells were observed in the pituitary of either control or Tg 10–1 mice (Fig. 3, C and D).

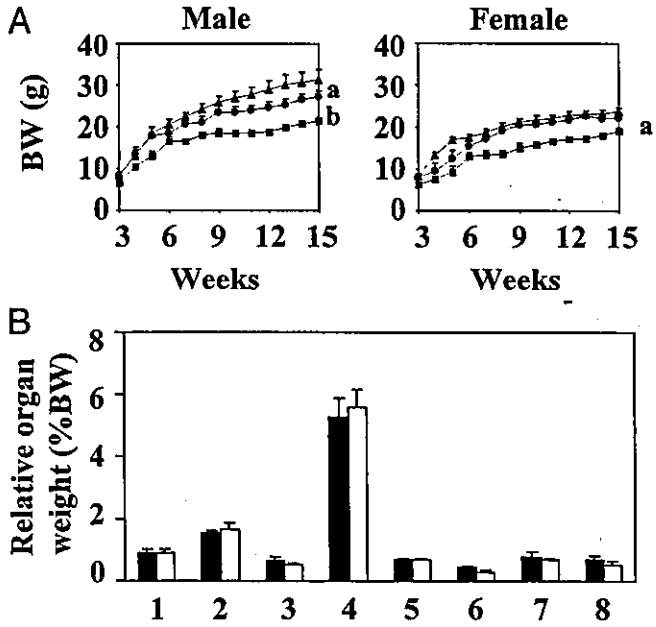

FIG. 2. Body weights (BW) and relative organ weights. A, Body weights of male (*left panel*) and female (*right panel*) control (*triangles*), Tg 9–2 (*circles*), and Tg 10–1 (*squares*) mice (n = 8/group). B, Relative organ weights of 8-wk-old control (*closed bars*) and Tg 10–1 (*open bars*) mice calculated from the organ and body weights (n = 8/group). 1, stomach; 2, cerebrum; 3, heart; 4, liver; 5, kidney; 6, spleen; 7, pancreas; 8, epididymal fat. a, $P < 0.05$; b, $P < 0.01$ (*vs.* control mice).

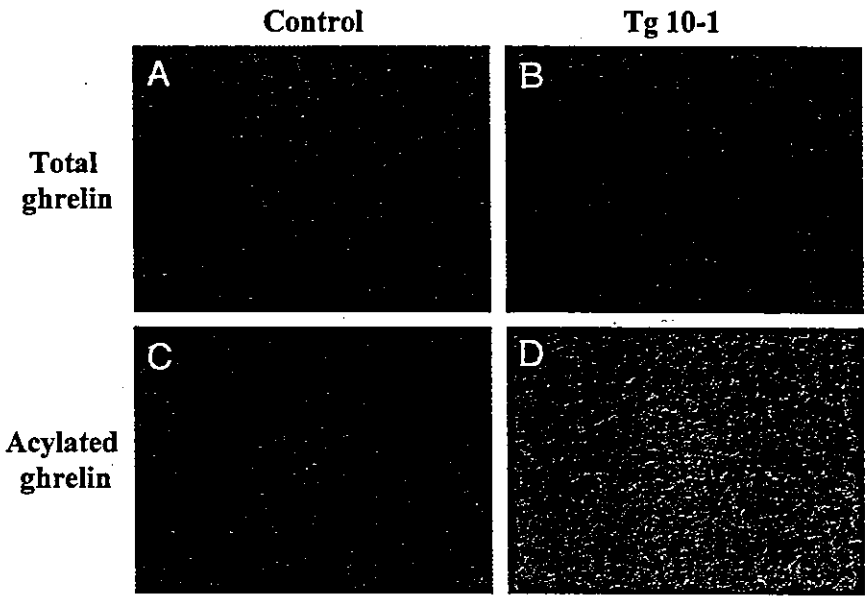

FIG. 3. The localization of total and acylated ghrelin-immunoreactive cells in the pituitary of 8-wk-old male control (A and C) and Tg 10–1 (B and D) mice. A and B, An antiserum raised to ghrelin(13–28) recognizing total (acylated plus des-acyl) ghrelin was used. C and D, An antiserum raised to ghrelin(1–11) specifically recognizing acylated ghrelin was used. Original magnification, ×40. The immunoreactive cells are stained *brown* by the avidin-biotin complex methods.

Food intake and biochemical parameters in the blood

Although absolute amounts of daily food intake were reduced in Tg 9–2 and Tg 10–1 mice, the amounts per body weight were not significantly changed in either male or female Tg 9–2 or Tg 10–1 mice, compared with control mice (Table 4). No significant differences in blood glucose, serum total protein, total cholesterol, and insulin levels were noted between 8-wk-old control and Tg 9–2 mice and control and Tg 10–1 mice (Table 4).

Serum GH, IGF-1, and pituitary GH mRNA levels

Serum GH levels in male control, Tg 9–2, and Tg 10–1 mice were 5.5 ± 1.9, 3.7 ± 0.7, and 2.3 ± 0.9 ng/ml, respectively (Fig. 4A). Those in female control, Tg 9–2, and Tg 10–1 mice were 4.7 ± 1.7, 2.5 ± 0.9, and 1.7 ± 0.8 ng/ml, respectively (Fig. 4A). There were tendencies for decline in serum GH levels in male and female Tg 9–2 and Tg 10–1 mice, compared with control mice, although the differences between them were not significant. Serum IGF-I levels in male control, Tg 9–2, and Tg 10–1 mice were 522 ± 23.6, 413.2 ± 49.0, and 364.1 ± 25.6 ng/ml, respectively (Fig. 4B). Those in male Tg 9–2 and Tg 10–1 mice were significantly reduced, compared with those in control mice ($P < 0.01$ for each). Serum IGF-I levels in female control, Tg 9–2, and Tg 10–1 mice were 509.7 ± 43.1, 545.5 ± 64.1, and 253.7 ± 36.4 ng/ml, respectively (Fig. 4B). Those in female Tg 10–1 mice were significantly reduced, compared with those in control mice ($P < 0.01$). The difference between female control and Tg 9–2 mice was not significant.

Pituitary GH mRNA levels in male control, Tg 9–2, and Tg 10–1 mice were 1.00, 0.62, and 0.42 AU, respectively. Those in Tg 9–2 and Tg 10–1 mice were significantly reduced, compared with those in control mice ($P < 0.05$ and $P < 0.01$, respectively). Pituitary GH mRNA levels in female control, Tg 9–2, and Tg 10–1 mice were 1.00, 0.97, and 0.71 AU. Those in female Tg 10–1 mice were significantly reduced, compared with those in control mice ($P < 0.05$). The difference between those in female control and Tg 9–2 mice was not significant (Fig. 4C).

Plasma ACTH, serum TSH, LH, and FSH levels

Plasma ACTH, serum TSH, LH, and FSH levels in 8-wk-old in male control and transgenic mice are shown in Table

TABLE 4. Daily food intake, blood glucose, serum total protein, total cholesterol, and insulin levels in 8-wk-old control and transgenic mice (n = 8/group)

	Control	Tg 9-2	Tg 10-1
Male			
Daily food intake (mg/BW/d)	149.1 ± 7.6	154.2 ± 3.2	155.2 ± 5.9
Serum total protein (mg/dl)	5.1 ± 0.2	4.9 ± 0.1	5.5 ± 0.1
Serum total cholesterol (mg/dl)	121.0 ± 12	116.9 ± 11.3	123.1 ± 8.3
Blood sugar (mg/dl)	134.2 ± 9.4	135.3 ± 8.7	136.7 ± 5.8
Serum insulin (pg/ml)	3233 ± 407	4624 ± 1015	2419 ± 423
Female			
Daily food intake (mg/BW/d)	167.5 ± 2.3	169.5 ± 4.7	165.8 ± 9.8
Serum total protein (mg/dl)	5.4 ± 0.1	5.1 ± 0.3	5.2 ± 0.3
Serum total cholesterol (mg/dl)	129.0 ± 9.3	123.4 ± 9.2	122.9 ± 6.1
Blood sugar (mg/dl)	132.1 ± 5.5	134.2 ± 6.4	130.6 ± 7.2
Serum insulin (pg/ml)	1182 ± 284	2079 ± 587	1799 ± 725

Values are given as the mean ± SEM. BW, Body weight.

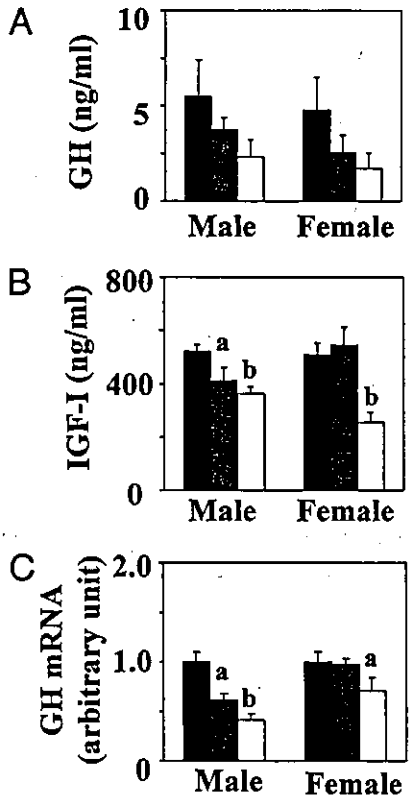

FIG. 4. Serum GH, IGF-I, and pituitary GH mRNA levels in 8-wk-old control (*closed bars*), Tg 9–2 (*shaded bars*), and Tg 10–1 (*open bars*) mice (n = 8/group). A, Serum GH levels. B, Serum IGF-I levels. C, Pituitary GH mRNA levels. a, $P < 0.05$; b, $P < 0.01$ (*vs.* control mice).

5. No significant difference was noted in the levels between control and transgenic mice.

Hematoxylin eosin and immunohistochemical staining for GH of the pituitary

Hematoxylin eosin staining is shown in Fig. 5, A and B. The pituitary morphology of Tg 10–1 mice was not different from that of the control mice. Immunohistochemical staining for GH is shown in Fig. 5, C and D. The distribution of GH-immunoreactive cells in the pituitary of Tg mice was similar to that of control mice.

Effects of GHRH and ghrelin on GH release

Control and Tg 10–1 mice were used. Serum GH levels after GHRH administration in male and female Tg 10–1 mice were similar to those of control mice throughout the course of the experiment (Fig. 6A). There was no significant difference in serum GH level at each time point between both male and female Tg-10 and control mice. Serum GH levels 10 min after ghrelin administration in male Tg10–1 and control mice were 63.1 ± 6.8 and 72.6 ± 12.0 ng/ml, respectively (Fig. 6B, *left panel*). The difference was not significant. Serum GH levels 20 min after ghrelin administration in male Tg10–1 and control mice were 30.2 ± 6.7 and 61.2 ± 15.5 ng/ml, respectively, and levels after 30 min were 11.8 ± 1.4 and 21.9 ± 4.1 ng/ml, respectively (Fig. 6B, *left panel*). Both differences were significant ($P < 0.01$). Serum GH levels 10 min after ghrelin administration in female Tg10–1 and control mice were 8.7 ± 3.7 and 52.8 ± 8.2 ng/ml, respectively, and those after 20 min were 29.8 ± 6.3 and 78.5 ± 14.3 ng/ml, respectively (Fig. 6B, *right panel*). Both differences were significant ($P < 0.01$). Serum GH levels 30 min after ghrelin administration in female Tg10–1 and control mice were 22.8 ± 6.3 and 22.3 ± 8.8 ng/ml, respectively (Fig. 6B, *right panel*). The difference was not significant.

TABLE 5. Plasma ACTH, serum TSH, LH, and FSH levels of 8-wk-old control and transgenic mice (n = 8/group)

	Control	Tg 9-2	Tg 10-1
ACTH (pg/ml)	135 ± 35	144 ± 32	123 ± 44
TSH (ng/ml)	3.31 ± 0.06	3.37 ± 0.11	3.49 ± 0.13
LH (ng/ml)	31.5 ± 2.1	30.8 ± 1.7	27.7 ± 2.1
FSH (ng/ml)	268.4 ± 21.8	221.1 ± 43.9	253.5 ± 24.6

Values are given as the mean ± SEM.

Expression of GHS-R in the pituitary

GHS-R mRNA levels of male control, Tg 9–2, and Tg 10–1 mice were 1.00, 1.56, and 3.46 AU, respectively (Fig. 7). The difference between control and Tg 10–1 mice was significant ($P < 0.01$).

Expression of hypothalamic neuropeptides that regulate GH secretion

GHRH mRNA levels of male control, Tg 9–2, and Tg 10–1 mice were 1.00, 0.88, and, 0.80 AU, respectively (Fig. 8A). The differences between control and Tg 9–2 mice and control and Tg 10–1 mice were not significant. Somatostatin mRNA levels of male control, Tg 9–2, and Tg 10–1 mice were 1.00, 1.08, and 0.97 AU, respectively (Fig. 8B). The differences between control and Tg 9–2 mice and control and Tg 10–1 mice were not significant.

Effects of continuous infusion of des-acyl ghrelin on GH-IGF-I axis and body weights

Male and female C57BL/6 mice were used. Serum GH levels after 10 d treatment with saline and des-acyl ghrelin in male mice were 5.8 ± 1.1 and 7.5 ± 2.0 ng/ml, respectively. The difference was not significant. Those with saline and des-acyl ghrelin in female mice were 9.2 ± 2.2 and 9.5 ± 1.8 ng/ml, respectively. The difference was not significant either. Serum IGF-I levels after 10 d treatment with saline and des-acyl ghrelin in male mice were 769.3 ± 16.6 and 768.7 ± 21.6 ng/ml, respectively. The difference was not significant. Those with saline and des-acyl ghrelin in female mice were 766.2 ± 13.4 and 719.4 ± 49.1 ng/ml, respectively. The difference was not significant either. Body weights and lengths in des-acyl ghrelin-injected mice were not significantly different from those in saline-injected mice in either males or females (data not shown).

Discussion

We have generated transgenic mouse lines that overexpress preproghrelin mRNA in a wide variety of tissues. The wide tissue distribution of preproghrelin mRNA in trans-

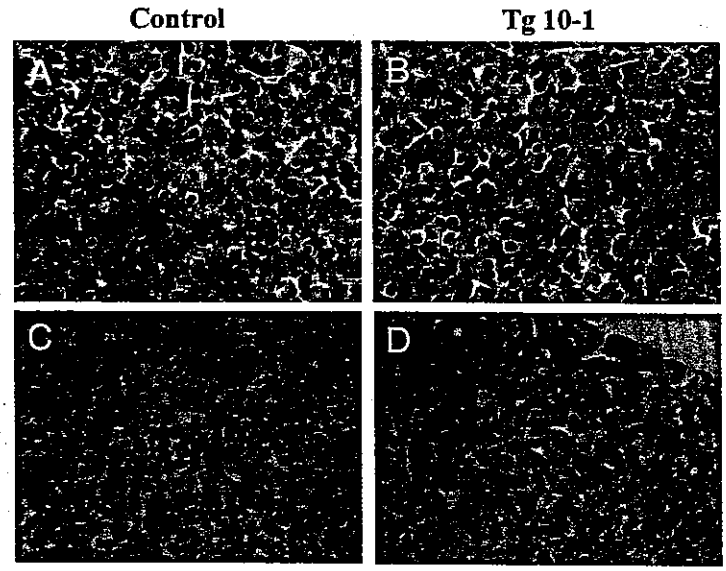

FIG. 5. Morphology of the pituitary and the localization of GH-immunoreactive cells in the pituitary of 8-wk-old male control (A and C) and Tg 10–1 (B and D) mice. A and B, Hematoxylin eosin (HE) staining. C and D, The localization of total and GH-immunoreactive cells in the pituitary. Original magnification, ×40. The immunoreactive cells are stained *brown* by the avidin-biotin complex methods.

genic mice was consistent with previous reports on transgenic mice using the CAG promoter (33, 34). Preproghrelin mRNA expression was increased, especially in Tg 10–1 mice, and its amount in the stomach reached 52-fold of that in control mice. Consistent with the elevated mRNA expression, peptide levels of total ghrelin (des-acyl plus acylated ghrelin) in various tissues were also elevated in transgenic mice. Plasma total ghrelin levels in transgenic mice showed marked results. Those in transgenic mice showed 10- and 44-fold of those in control mice. We originally intended to generate mice overexpressing biologically active ghrelin. Unexpectedly, acylated ghrelin levels were not changed in all tissues examined and plasma of transgenic mice, compared with those of control mice, indicating that transgenic mice overexpress only des-acyl ghrelin. The expression of acylated ghrelin has been reported in a small number of tissues, such as the stomach (X/A cells), duodenum, hypothalamus, and pancreatic α-cells (1, 31, 39, 40). These reports and our present data suggest that only a limited number of cell lineages may able to process proghrelin or acylate ghrelin. The underlying mechanism by which ghrelin is acylated is unknown to date. Further study is needed to clarify the mechanism of the acylation.

The acylation of ghrelin is assumed to be essential for its actions, and des-acyl ghrelin, which lacks the modification, is devoid of endocrine actions, based on previous studies (1, 41). However, recent studies indicated that des-acyl ghrelin may have some actions. Des-acyl ghrelin as well as acylated ghrelin causes a significant inhibition of cell proliferation in human breast carcinoma cell lines (29) and inhibits cell death in cardiomyocytes and endothelial cells through ERK1/2 and phosphatidylinositol 3-kinase/AKT (30). In addition, one study (42) reported that acylated and des-acyl ghrelin promote adipogenesis directly *in vivo* by a mechanism independent of known GHS-Rs. Moreover, another study (28) indicated that des-acyl ghrelin may offset the action of acylated ghrelin on insulin secretion. Ghrelin has been shown to induce a reduction in serum insulin levels. In the study, coadministration of acylated plus des-acyl ghrelin did not re-

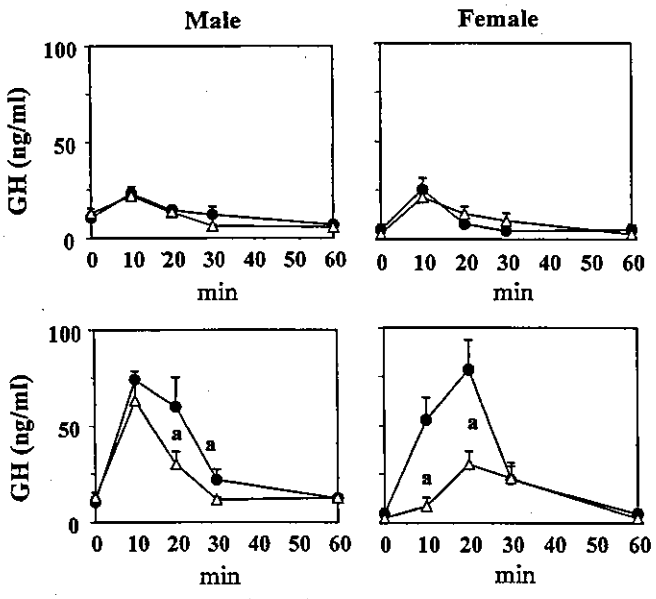

FIG. 6. The responses of GH to GHRH and ghrelin in 8-wk-old control (*closed circles*) and Tg 10–1 (*open triangles*) mice. A, Time course of serum GH levels after iv injection of 60 μg/kg GHRH (n = 8/each point). B, Time course of serum GH levels after iv injection of 40 μg/kg ghrelin (n = 8/each point). a, $P < 0.01$ (*vs.* control mice).

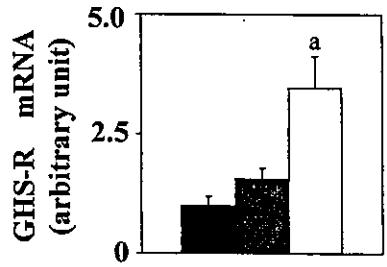

FIG. 7. Pituitary GHS-R mRNA levels in 8-wk-old control (*closed bars*), Tg 9–2 (*shaded bars*), and Tg 10–1 (*open bars*) mice quantified by real-time PCR analysis (n = 8/group). a, $P < 0.01$ (*vs.* control mice).

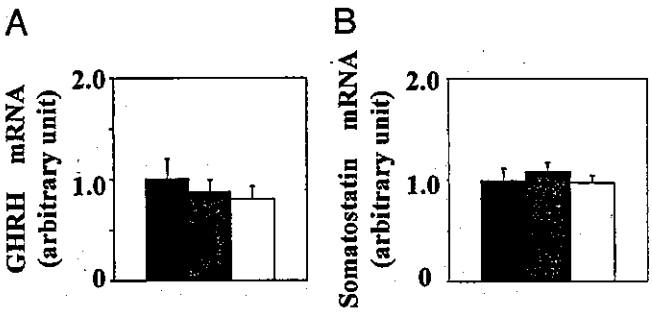

FIG. 8. Hypothalamic GHRH and somatostatin mRNA levels in 8-wk-old control (*closed bars*), Tg 9–2 (*shaded bars*), and Tg 10–1 (*open bars*) mice quantified by real-time PCR analysis. A, GHRH mRNA levels (n = 8/group). B, Somatostatin mRNA levels (n = 8/group).

sult in any changes in serum insulin levels in humans, suggesting that ghrelin action on insulin is modulated by des-acyl ghrelin.

The present study indicates that transgenic mice overexpressing des-acyl ghrelin show small phenotype. Longitudinal growth was the most reduced in female Tg 10–1 mice (20% reduction from control mice). The phenotype was not associated with changes in BMIs. These mice did not show decreased food intake or decreased body fat mass. In addition, they showed normal nutritional condition, based on their biochemical parameters, including blood glucose, serum total protein, and total cholesterol levels. These data indicate that the small phenotype of transgenic mice is not attributed to poor nutritional condition.

Serum IGF-I levels were significantly reduced in male and female transgenic mice, compared with control mice. Female Tg 10–1 mice had no less than 50% reduction in serum IGF-I levels, compared with control mice. Although the differences in serum GH levels between control and transgenic mice were not statistically significant, probably because of the pulsatile character of GH secretion, the levels tended to be reduced in transgenic mice, compared with control mice, and the mean GH level of Tg10–1 mice was only 50% of that of control mice. It should be emphasized that Tg 10–1 mice showed lower serum GH levels than Tg 9–2 mice. Body weights and lengths of the former were more reduced than the latter. It should be also noted that the former showed higher des-acyl ghrelin expression than the latter. Reduced pituitary GH mRNA levels in transgenic mice support the observation. The GH-IGF-I axis-specific alteration in transgenic mice was also indicated by the measurement of other anterior pituitary hormones than GH. Plasma ACTH, serum TSH, LH, and FSH levels were not altered.

The size and morphology of the pituitary including the somatotrope populations of transgenic mice were similar to those of control mice. These data indicated that there is no apparent change, suggesting developmental problems in the pituitary of transgenic mice.

Responses of GH to GHRH and ghrelin in transgenic mice exhibited intriguing results. Transgenic mice showed normal response of GH to GHRH. Alternatively, if we consider that the basal GH levels are lower in transgenic mice, the similar maximal response might indicate that they are hyperresponsive to GHRH. It is not likely that an insufficient dose of GHRH induced submaximal response of GH in both control and transgenic mice, judging from previous reports (43). On the other hand, the responses of GH to ghrelin were reduced in transgenic mice. It is noteworthy that the reduction was much greater in female transgenic mice than in male mice, if we take their serum IGF-I levels into account. Taken together our results and these reports indicate that overexpression of des-acyl ghrelin in our mice may result in reduction of GH response to endogenous ghrelin, and it may result in the reduced serum IGF-I levels in transgenic mice.

The reduced GH response to ghrelin in transgenic mice could be due to down-regulated the GHS-R. However, the pituitary GHS-R mRNA levels in the transgenic mice were rather elevated. It is not likely that overexpressed des-acyl ghrelin acts as a blocking agent to the GHS-R because ^{125}I-labeled acylated ghrelin bound to the GHS-R cannot be displaced by des-acyl ghrelin (20). Overexpressed des-acyl ghrelin may have some effects on endogenous GH secretion, modifying the action of endogenous ghrelin in transgenic mice via, for instance, another receptor or modulation of the signal transduction pathway after the GHS-R.

Previous reports indicated that the hypothalamus plays a critical role in the stimulatory effect of ghrelin on GH secretion as well as the pituitary (21, 22, 23). Because GH secretion is regulated chiefly by two hypothalamic hormones, GHRH and somatostatin, the expression of these hormones could be altered in transgenic mice. We could not find any significant difference in either GHRH or somatostatin mRNA levels between control and transgenic mice. These data might suggest that overexpressed des-acyl ghrelin acts on not only the pituitary but also the hypothalamus in the transgenic mice, judging from the fact that hypothalamus GHRH mRNA were not elevated, and somatostatin mRNA levels were not decreased despite the decreased serum GH levels.

We could not show, unfortunately, that continuous ip infusion of des-acyl ghrelin has some effect on serum GH and IGF-I levels or body weights. It should be noted, however, that plasma des-acyl ghrelin levels in transgenic mice reached 10- and 50-fold of those in control mice. Administration of a higher dose of des-acyl ghrelin, or longer administration, might result in alteration in the GH-IGF-I axis. On the other hand, the phenotype of transgenic mice might reflect direct effects of ubiquitous expression of des-acyl ghrelin. It should also be noted that high levels of des-acyl ghrelin were detected in a various tissues, especially in the pituitary, as well as in plasma of transgenic mice. The des-acyl ghrelin immunoreactive pituitary cells might play an important role in the mechanism for the altered GH-IGF-I axis in a paracrine or autocrine manner. It should be pointed out that preproghrelin mRNA is reported to be expressed in the normal pituitary (44), as we showed in the present study, suggesting its physiological role in GH secretion. The phenotype of transgenic mice may reflect the role. Further study is needed for this issue.

The mechanism underlying the sexual dimorphism in the responses of GH to ghrelin in transgenic mice is not fully understood. It might be due to the gender difference in the secretory regulation of GH. Female mice have been reported to be different from male mice in that they have noncyclical

and rather low somatostatin output and that GHRH plays a dominant role in it (45). There might be a GHRH-dependent mechanism for the reduced response in transgenic mice. Indeed, one recent report (26) indicated that transgenic rats expressing an antisense GHS-R mRNA in the hypothalamic arcuate nucleus show marked gender difference in GH secretion. Although there was no significant difference in pulse frequency and baseline levels of GH between male control and transgenic rats, female transgenic rats showed lower baseline levels and fewer pulses of GH than female control rats (26).

The 94-amino acid proghrelin is cleaved to yield ghrelin. One previous study (46) demonstrated that C-terminal proghrelin peptides are present in the human circulation. Transgenic mice in the present study would also overexpress these peptides. We have not excluded the possibility that the phenotype of transgenic mice might be due to the effects of these peptides.

In conclusion, the present study demonstrates that transgenic mice overexpressing des-acyl ghrelin show small phenotype and altered GH-IGF-I axis. These observations may indicate a role of des-acyl ghrelin in the regulation of GH secretion.

Acknowledgments

The authors gratefully acknowledge the excellent technical support of Chieko Ishimoto and Hitomi Hiratani.

Received May 17, 2004. Accepted October 1, 2004.

Address all correspondence and requests for reprints to: Kazuhiko Takaya, M.D., Ph.D., Translational Research Center, Kyoto University Hospital, Kyoto 606-8507, Japan. E-mail: ktakaya@kuhp.kyoto-u.ac.jp.

This work was supported by research grants from the Japanese Ministry of Education, Science, and Culture and the Japanese Ministry of Health, Labor, and Welfare.

References

1. Kojima M, Hosoda H, Date Y, Nakazato M, Matsuo H, Kangawa K 1999 Ghrelin is a growth-hormone-releasing acylated peptide from stomach. Nature 402:656–660
2. Date Y, Murakami N, Kojima M, Kuroiwa T, Matsukura S, Kangawa K, Nakazato M 2000 Central effects of a novel acylated peptide, ghrelin, on growth hormone release in rats. Biochem Biophys Res Commun 275:477–480
3. Ariyasu H, Takaya K, Tagami T, Ogawa Y, Hosoda K, Akamizu T, Suda M, Koh T, Natsui K, Toyooka S, Shirakami G, Usui T, Shimatsu A, Doi K, Hosoda H, Kojima M, Kangawa K, Nakao K 2001 Stomach is a major source of circulating ghrelin, and feeding state determines plasma ghrelin-like immunoreactivity levels in humans. J Clin Endocrinol Metab 86:4753–4758
4. Lu S, Guan JL, Wang QP, Uehara K, Yamada S, Goto N, Date Y, Nakazato M, Kojima M, Kangawa K, Shioda S 2001 Immunocytochemical observation of ghrelin-containing neurons in the rat arcuate nucleus. Neurosci Lett 321: 157–160
5. Cowley MA, Smith RG, Diano S, Tschop M, Pronchuk N, Grove KL, Strasburger CJ, Bidlingmaier M, Esterman M, Heiman ML, Garcia-Segura LM, Nillni EA, Mendez P, Low MJ, Sotonyi P, Friedman JM, Liu H, Pinto S, Colmers WF, Cone RD, Horvath TL 2003 The distribution and mechanism of action of ghrelin in the CNS demonstrates a novel hypothalamic circuit regulating energy homeostasis. Neuron 37:649–661
6. Cummings DE, Purnell JQ, Frayo RS, Schmidova K, Wisse BE, Weigle DS 2001 A preprandial rise in plasma ghrelin levels suggests a role in meal initiation in humans. Diabetes 50:1714–1719
7. Asakawa A, Inui A, Kaga T, Yuzuriha H, Nagata T, Ueno N, Makino S, Fujimiya M, Niijima A, Fujino MA, Kasuga M 2001 Ghrelin is an appetite-stimulatory signal from stomach with structural resemblance to motilin. Gastroenterology 120:337–345
8. Nakazato M, Murakami N, Date Y, Kojima M, Matsuo H, Kangawa K, Matsukura S 2001 A role for ghrelin in the central regulation of feeding. Nature 409:194–198
9. Ariyasu H, Takaya K, Hosoda H, Iwakura H, Ebihara K, Mori K, Ogawa Y, Hosoda K, Akamizu T, Kojima M, Kangawa K, Nakao K 2002 Delayed short-term secretory regulation of ghrelin in obese animals: evidenced by a specific RIA for the active form of ghrelin. Endocrinology 143:3341–3350
10. Tschop M, Weyer C, Tataranni PA, Devanarayan V, Ravussin E, Heiman ML 2001 Circulating ghrelin levels are decreased in human obesity. Diabetes 50: 707–709
11. Hanada T, Toshinai K, Kajimura N, Nara-Ashizawa N, Tsukada T, Hayashi Y, Osuye K, Kangawa K, Matsukura S, Nakazato M 2003 Anti-cachectic effect of ghrelin in nude mice bearing human melanoma cells. Biochem Biophys Res Commun 301:275–279
12. Shintani M, Ogawa Y, Ebihara K, Aizawa-Abe M, Miyanaga F, Takaya K, Hayashi T, Inoue G, Hosoda K, Kojima M, Kangawa K, Nakao K 2001 Ghrelin, an endogenous growth hormone secretagogue, is a novel orexigenic peptide that antagonizes leptin action through the activation of hypothalamic neuropeptide Y/Y1 receptor pathway. Diabetes 50:227–232
13. Wren AM, Small CJ, Abbott CR, Dhillo WS, Seal IJ, Cohen MA, Batterham RL, Taheri S, Stanley SA, Ghatei MA, Bloom SR 2001 Ghrelin causes hyperphagia and obesity in rats. Diabetes 50:2540–2547
14. Dieguez C, Casanueva FF 2000 Ghrelin: a step forward in the understanding of somatotroph cell function and growth regulation. Eur J Endocrinol 142: 413–417
15. Seoane LM, Tovar S, Baldelli R, Arvat E, Ghigo E, Casanueva FF, Dieguez C 2000 Ghrelin elicits a marked stimulatory effect on GH secretion in freely moving rats. Eur J Endocrinol 143:R7–R9
16. Takaya K, Ariyasu H, Kanamoto N, Iwakura H, Yoshimoto A, Harada M, Mori K, Komatsu Y, Usui T, Shimatsu A, Ogawa Y, Hosoda K, Akamizu T, Kojima M, Kangawa K, Nakao K 2000 Ghrelin strongly stimulates growth hormone release in humans. J Clin Endocrinol Metab 85:4908–4911
17. Guan XM, Yu H, Palyha OC, McKee KK, Feighner SD, Sirinathsinghji DJ, Smith RG, Van der Ploeg LH, Howard AD 1997 Distribution of mRNA encoding the growth hormone secretagogue receptor in brain and peripheral tissues. Brain Res Mol Brain Res 48:23–29
18. Gnanapavan S, Kola B, Bustin SA, Morris DG, McGee P, Fairclough P, Bhattacharya S, Carpenter R, Grossman AB, Korbonits M 2002 The tissue distribution of the mRNA of ghrelin and subtypes of its receptor, GHS-R, in humans. J Clin Endocrinol Metab 87:2988
19. Willesen MG, Kristensen P, Romer J 1999 Co-localization of growth hormone secretagogue receptor and NPY mRNA in the arcuate nucleus of the rat. Neuroendocrinology 70:306–316
20. Muccioli G, Papotti M, Locatelli V, Ghigo E, Deghenghi R 2001 Binding of ^{125}I-labeled ghrelin to membranes from human hypothalamus and pituitary gland. J Endocrinol Invest 24:RC7–RC9
21. Torsello A, Grilli R, Luoni M, Guidi M, Ghigo MC, Wehrenberg WB, Deghenghi R, Muller EE, Locatelli V 1996 Mechanism of action of hexarelin. I. Growth hormone-releasing activity in the rat. Eur J Endocrinol 135:481–488
22. Maheshwari HG, Rahim A, Shalet SM, Baumann G 1999 Selective lack of growth hormone (GH) response to the GH-releasing peptide hexarelin in patients with GH-releasing hormone receptor deficiency. J Clin Endocrinol Metab 84:956–959
23. Hataya Y, Akamizu T, Takaya K, Kanamoto N, Ariyasu H, Saijo M, Moriyama K, Shimatsu A, Kojima M, Kangawa K, Nakao K 2001 A low dose of ghrelin stimulates growth hormone (GH) release synergistically with GH-releasing hormone in humans. J Clin Endocrinol Metab 86:4552–4555
24. Okimura Y, Ukai K, Hosoda H, Murata M, Iguchi G, Iida K, Kaji H, Kojima M, Kangawa K, Chihara K 2003 The role of circulating ghrelin in growth hormone (GH) secretion in freely moving male rats. Life Sci 72:2517–2524
25. Sun Y, Ahmed S, Smith RG 2003 Deletion of ghrelin impairs neither growth nor appetite. Mol Cell Biol 23:7973–7981
26. Shuto Y, Shibasaki T, Otagiri A, Kuriyama H, Ohata H, Tamura H, Kamegai J, Sugihara H, Oikawa S, Wakabayashi I 2002 Hypothalamic growth hormone secretagogue receptor regulates growth hormone secretion, feeding, and adiposity. J Clin Invest 109:1429–1436
27. Hosoda H, Kojima M, Matsuo H, Kangawa K 2000 Ghrelin and des-acyl ghrelin: two major forms of rat ghrelin peptide in gastrointestinal tissue. Biochem Biophys Res Commun 279:909–913
28. Broglio F, Prodam F, Benso A, Gottero C, Destefanis S, Gauna C, van der Lely AJ, Ghigo E, The peripheral but not the neuro-endocrine response to acylated ghrelin is modulated by non-acylated ghrelin in humans. Program of the 85th Annual Meeting of The Endocrine Society, Philadelphia, PA, 2003, p 264 (Abstract P1-553)
29. Cassoni P, Papotti M, Ghe C, Catapano F, Sapino A, Graziani A, Deghenghi R, Reissmann T, Ghigo E, Muccioli G 2001 Identification, characterization, and biological activity of specific receptors for natural (ghrelin) and synthetic growth hormone secretagogues and analogs in human breast carcinomas and cell lines. J Clin Endocrinol Metab 86:1738–1745
30. Baldanzi G, Filigheddu N, Cutrupi S, Catapano F, Bonissoni S, Fubini A, Malan D, Baj G, Granata R, Broglio F, Papotti M, Surico N, Bussolino F, Isgaard J, Deghenghi R, Sinigaglia F, Prat M, Muccioli G, Ghigo E, Graziani A 2002 Ghrelin and des-acyl ghrelin inhibit cell death in cardiomyocytes and endothelial cells through ERK1/2 and PI 3-kinase/AKT. J Cell Biol 159:1029–1037
31. Iwakura H, Hosoda K, Doi R, Komoto I, Nishimura H, Son C, Fujikura J,

Tomita T, Takaya K, Ogawa Y, Hayashi T, Inoue G, Akamizu T, Hosoda H, Kojima M, Kangawa K, Imamura M, Nakao K 2002 Ghrelin expression in islet cell tumors: augmented expression of ghrelin in a case of glucagonoma with multiple endocrine neoplasm type I. J Clin Endocrinol Metab 87:4885–4888

32. Mori K, Yoshimoto A, Takaya K, Hosoda K, Ariyasu H, Yahata K, Mukoyama M, Sugawara A, Hosoda H, Kojima M, Kangawa K, Nakao K 2000 Kidney produces a novel acylated peptide, ghrelin. FEBS Lett 486:213–216
33. Ikawa M, Kominami K, Yoshimura Y, Tanaka K, Nishimune Y, Okabe M 1995 Green fluorescent protein as a marker in transgenic mice. Dev Growth Differ 37:455–459
34. Niwa H, Yamamura K, Miyazaki J 1991 Efficient selection for high-expression transfectants with a novel eukaryotic vector. Gene 108:193–199
35. Ogawa Y, Masuzaki H, Hosoda K, Aizawa-Abe M, Suga J, Suda M, Ebihara K, Iwai H, Matsuoka N, Satoh N, Odaka H, Kasuga H, Fujisawa Y, Inoue G, Nishimura H, Yoshimasa Y, Nakao K 1999 Increased glucose metabolism and insulin sensitivity in transgenic skinny mice overexpressing leptin. Diabetes 48:1822–1829
36. Bahary N, Leibel RL, Joseph L, Friedman JM 1990 Molecular mapping of the mouse db mutation. Proc Natl Acad Sci USA 87:8642–8646
37. Maffei M, Halaas J, Ravussin E, Pratley RE, Lee GH, Zhang Y, Fei H, Kim S, Lallone R, Ranganathan S 1995 Leptin levels in human and rodent: measurement of plasma leptin and ob RNA in obese and weight-reduced subjects. Nat Med 1:1155–1161
38. Chomczynski P, Sacchi N 1987 Single-step method of RNA isolation by acid guanidinium thiocyanate-phenol-chloroform extraction. Anal Biochem 162: 156–159
39. Date Y, Kojima M, Hosoda H, Sawaguchi A, Mondal MS, Suganuma T, Matsukura S, Kangawa K, Nakazato M 2000 Ghrelin, a novel growth hormone-releasing acylated peptide, is synthesized in a distinct endocrine cell type in the gastrointestinal tracts of rats and humans. Endocrinology 141: 4255–4261
40. Date Y, Nakazato M, Hashiguchi S, Dezaki K, Mondal MS, Hosoda H, Kojima M, Kangawa K, Arima T, Matsuo H, Yada T, Matsukura S 2002 Ghrelin is present in pancreatic α-cells of humans and rats and stimulates insulin secretion. Diabetes 51:124–129
41. Broglio F, Benso A, Gottero C, Prodam F, Gauna C, Filtri L, Arvat E, van der Lely AJ, Deghenghi R, Ghigo E 2003 Non-acylated ghrelin does not possess the pituitaric and pancreatic endocrine activity of acylated ghrelin in humans. J Endocrinol Invest 26:192–196
42. Thompson NM, Gill DA, Davies R, Loveridge N, Houston PA, Robinson IC, Wells T 2004 Ghrelin and des-octanoyl ghrelin promote adipogenesis directly *in vivo* by a mechanism independent of the type 1a growth hormone secretagogue receptor. Endocrinology 145:234–242
43. Clark RG, Robinson IC 1985 Effects of a fragment of human growth hormone-releasing factor in normal and 'little' mice. J Endocrinol 106:1–5
44. Kamegai J, Tamura H, Shimizu T, Ishii S, Sugihara H, Oikawa S 2001 Regulation of the ghrelin gene: growth hormone-releasing hormone upregulates ghrelin mRNA in the pituitary. Endocrinology 142:4154–4157
45. Robinson IC 1991 The growth hormone secretory pattern: a response to neuroendocrine signals. Acta Paediatr Scand Suppl 372:70–78;discussion 79–80
46. Pemberton C, Wimalasena P, Yandle T, Soule S, Richards M 2003 C-terminal pro-ghrelin peptides are present in the human circulation. Biochem Biophys Res Commun 310:567–573

Endocrinology is published monthly by The Endocrine Society (http://www.endo-society.org), the foremost professional society serving the endocrine community.